Elsevier Editorial System(tm) for Journal of Hydrology
Manuscript Draft

Manuscript Number:

Title: Assessing the long-term dynamics and nutrient loads to an eutrophic reservoir in a temporary river basin in southeast Portugal (Enxoé)

Article Type: Research Paper

Keywords: Enxoé, eutrophic reservoir, nutrients, watershed modeling, SWAT model

Corresponding Author: Mr. David Brito,

Corresponding Author's Institution: Maretec - Instituto Superior Técnico - Technical University of Lisbon, Av. Rovisco Pais, 1049-001 Lisboa, Portugal

First Author: David Brito

Order of Authors: David Brito; Ramiro Neves; Maria A Branco; Ângela Prazeres; Sara Rodrigues; Maria C Gonçalves; Tiago B Ramos

Suggested Reviewers: Jirka Simunek Ph.D.
Knowledge on nutrient modelling with Hidrus

Francesc Gallart Ph.D.
Surface Hydrology and Erosion Group, Geosciences Department Institute of Environ, CSIC
francesc.gallart@idaea.csic.es
knowledge on hydrology processes and semi-arid temporary watersheds

Ragahavan Srinivasan Ph.D.
Spatial Science Laboratory, Texas A & M University
in depth knowledge on SWAT modelling on hydrology and water quality

Antonio Lo Porto Ph.D.
Istituto di Ricerca sulle Acque, Consiglio Nazionale delle Ricerche
in depth knowledge about SWAT and watershed modelling and management.

Laurent Charlet
Editor in chief of similar themed articles

Chong-Yu Xu
Associate editor of similar themed articles

Sheng Yue
Associated Editor of similar themed articles

Martin Beniston
Associated Editor of similar themed articles

Bernhard Wehrli

Associated Editor of similar themed articles

ASSESSING THE LONG-TERM DYNAMICS AND NUTRIENT LOADS TO AN EUTROPHIC RESERVOIR IN A TEMPORARY RIVER BASIN IN SOUTHEAST PORTUGAL (ENXOÉ)

David Brito[1]; Ramiro Neves[1]; Maria A. Branco[2], Ângela Prazeres[2], Sara Rodrigues[2], Maria C. Gonçalves[2], Tiago B. Ramos[3]

[1] Maretec, Instituto Superior Técnico, Technical University of Lisbon, Av. Rovisco Pais, 1049-001 Lisboa, Portugal.

[2] Instituto Nacional de Recursos Biológicos, Quinta do Marquês, Av. República, 2784-505 Oeiras, Portugal.

[3] CEER-Biosystems Engineering, Institute of Agronomy, Technical University of Lisbon, Tapada da Ajuda, 1349-017 Lisboa, Portugal.

First author and corresponding author: David Brito, e-mail: david.maretec@ist.utl.pt, tel: 00351 218419425

Abstract

The Enxoé reservoir was built in 1998 (with a total capacity of 10 hm^3). Since 2000, it has exhibited frequent high chlorophyll-a concentrations (reaching a geometric mean 6 times the national limit for eutrophication of 10 $\mu g.L^{-1}$) and represents the reservoir with the highest eutrophic state in Portugal. Toxic algal blooms have also been observed in this reservoir, and these blooms pose serious challenges to water managers because the reservoir is used for potable water production. In an effort to contribute to the reduction of the trophy state, the watershed input was characterized, and the following approach was used: i) collect data in the ungauged watershed (during the period 2010-2011); ii) implement the SWAT model and validate it against field data; and iii) extrapolate the results to the basin scale and characterize the watershed dynamics (water and nutrient balances). The SWAT estimates of the simulated flow and nutrient loads were in good agreement with field data (monthly flow with R^2 and Nash-Sutcliffe efficiencies > 0.75 and nutrient loads from 0.62 to 0.70). At the basin scale over a 30 year period, the average annual values show that approximately 15-20% of the annual precipitation (approximately 500 mm) is routed to the river (80-85% evapotranspiration). Moreover, the nutrient exports to the river for total nitrogen were on the order of 2.5-2.8 $kg.ha^{-1}.year^{-1}$, suspended solids exports were 0.45 $ton.ha^{-1}.year^{-1}$ and total phosphorus exports were 0.4 $kg.ha^{-1}.year^{-1}$; these results are consistent with the gentle slopes, extensive agricultural activities and low urban pressure associated with Enxoé. The “normal” order of magnitude in nutrient exports from the watershed suggests that the reservoir eutrophication may be linked also to the reservoir geometry (average depth of 5 m), which provides high light availability to the bottom sediments. Further work should

integrate the SWAT model results into a reservoir model to depict the origin of the Enxoé trophic state and test management scenarios that may reduce it.

Keywords: Enxoé, eutrophic reservoir, nutrients, watershed modeling, SWAT model

1 Introduction

The Enxoé reservoir was built in 1998, and since 2000, it has had frequent chlorophyll-a concentrations higher than 50 $\mu g.L^{-1}$. The geometric average of the surface chlorophyll-a concentration in the period of 1998-2009 measured from April to September was approximately 60 $\mu g.L^{-1}$, whereas the national limit for eutrophication is 10 $\mu g.L^{-1}$. Moreover, toxic cyanobacteria blooms occurred (INAG, 2004 and Valerio et. al. 2005) and interrupted water distribution to the local population. This situation is a problem for water management for two reasons: i) the eutrophication of the reservoir in the scope of the Water Framework Directive calls for management plans, and ii) the high concentration of algae and, specifically, the presence of toxic algae is a major issue in a reservoir that is used for water production.

Cyanobacteria algae dominance is usually described by two main processes: i) some species are able to consume N_2 dissolved in water (Paerl et al. 2001, Havens et al. 2003, Rolff et al. 2007), whereas ii) some species are able to maintain growth even under conditions of low light availability (Havens et al. 2003). The nitrogen fixation characteristic of some types of cyanobacteria allows them to be independent of the availability of inorganic forms of nitrogen (e.g., ammonia, nitrate). Furthermore, under conditions of nitrogen limitation, cyanobacteria have the potential to generate blooms if phosphorus is available (Havens, 2003).

Such a cyanobacterial response to phosphorus availability may have occurred in Enxoé reservoir after 2002 when these species started to be dominant (INAG, 2004, Coelho et al. 2008). 2000/2001 was a wet hydrologic year, and the winter floods transported adsorbed

material to the reservoir. The first blooms consumed the available inorganic material while organic matter deposited. The accumulation of organic matter at the bottom of the reservoir and the corresponding increase in mineralization may have depleted the oxygen near the bottom (where mineralization is more intense); thus, under anoxic conditions, phosphorus may have been released from the absorbed phase to the water column (Lake et al. 2007, Jiang et al. 2006) and fueled blooms. These processes were noted in previous work performed at Enxoé as the probable drivers for algal blooms in Enxoé and also for cyanobacterial dominance (Coelho et al. 2008).

Previous work focused on Enxoé linked the cyanobacteria blooms in the reservoir to the input loads from the watershed and that such blooms could be associated with phosphorus input. Phosphorus feeding from the watershed may have fueled the process, which consists of both a fast and a delayed response in the reservoir (initial blooms arise from the consumption of input dissolved nutrients, while later blooms are attributable to sediment sources, e.g., mineralization and dessortion under anoxic conditions; (Coelho et al. 2008). Usually, phosphorus is transported in the watershed cycle and is adsorbed onto fine particles associated with erosion. Previous studies noted the need to understand the role of erosion and phosphorus input in Enxoé reservoir blooms.

The approach needed to understand the Enxoé trophic state must integrate the watershed and the reservoir to determine the impact in the reservoir of management responses on the watershed (e.g., changes in agricultural practices, reducing erosion, etc.). The ultimate objective includes coupling a watershed model and a reservoir model (integrating the available data) to determine the best-suited management strategies (in the watershed and/or reservoir) to reduce the reservoir trophic status. This article focuses on the first

97 part: understanding the watershed dynamics and quantifying the nutrient feeding to the
98 reservoir.
99 The SWAT model was used for watershed characterization of the long-term fluxes to the
100 reservoir. The SWAT model has been widely applied to a range of watershed sizes and
101 configurations to simulate flow and nutrient export on daily, monthly and annual scales
102 (Gassman et al. 2007, Zhang et al. 2008). Examples of such implementation in small-
103 sized and similar land uses as Enxoé include the work of Geza and McCray, (2008) and
104 Green and van Griensven, (2008) both in USA, applications in Portuguese watersheds
105 (e.g., for nitrogen export in Roxo, Yevenes and Mannaerts, 2011) or in other semi-arid
106 Mediterranean watersheds in Spain and Greece (e.g., Dechmi et al. 2012, Panagopoulos
107 et al. 2011). SWAT model have also been successfully linked to the reservoir model CE-
108 QUAL-W2 for water quality management (e.g., Debele et al. 2005).
109 To estimate the input loads to the Enxoé reservoir, the SWAT model was used, and
110 because the Enxoé basin was ungauged, field data were collected from 2010 to 2011 to
111 validate the model.
112

2 Material and Methods

2.1 Study area

Enxoé is a 60 km^2 watershed located in southeast Portugal in the left margin of the Guadiana River (Figure 1). The main river is Ribeira do Enxoé, which has a length of approximately 10 km from its headwaters to the reservoir. The Enxoé reservoir wall's approximate coordinates are 37º 59' 38.121" N, 7º 27' 54.776" W. The reservoir has a total volume of 10.4 hm^3, a surface area approximately 2 km^2 and an average depth of 5 m.

Enxoé has an annual average precipitation of 500 mm and is a temporary river, with flow in the winter as a response to rain events, decreasing flow in the spring after the rain ceases and no flow and pool formation during the summer or in low-flow conditions. The slopes are low, with an average river slope of approximately 2%; the watershed has an average slope of 5-6%. The existence of low slopes and some flatter areas promotes water pooling and the occurrence of disconnected flows.

The land in Enxoé is mainly used for olive trees, oak-pasture mixed system ("montado") and annual crops (each with approximately 30% of the total area) - Figure 2 and Table 3. The annual crops are wheat, oats and sunflowers.

The soil in Enxoé originates mainly from granite and limestone (each with approximately 30% of the total area) and schist (with approximately 10% of the total area).

Approximately 1000 inhabitants live in the Enxoé watershed (mostly in the only village, Vale de Vargo), and the Waste Water Treatment Plan (WWTP) that has served the

population, since 2006 discharges outside the watershed as a protective measure to the Enxoé reservoir.

The extensive production of cows and sheep is the most important animal-farming activity in Enxoé. According to the 1999 agricultural census (INE – Instituto Nacional de Estatística), there were approximately 600 cows (10 per km^2) and 4200 sheep (70 per km^2) in the catchment.

The Enxoé watershed was ungauged; thus, to quantify the nutrient export and validate the model, field activities were conducted in 2010 and 2011: river sampling in the two main tributaries, and the installation of erosion plots for two of the main uses - olive trees and "montado" (Figure 1).

2.2 SWAT model description

SWAT is a basin-scale, distributed and continuous-time model, and its land hydrodynamic component solves water balance and relates the meteorological variables with the basin features (topography, soil type and land use). In water quality component, plant growth, nitrogen and phosphorus soil cycles, sediment and pesticides transport, are simulated (Neitsch et al. 2002).

The SWAT model divides the watershed into sub-basins and into HRU (hydrological response units) that are homogeneous in terms of soil, land use and slope (the basic computation units) and soil may be divided into vertical layers.

The SWAT model hydrology solves for the soil, the water balance between the infiltration/runoff generation (e.g. the modified SCS curve number method), percolation (if the water content is higher than the field capacity), lateral flow (dependent on slope),

158 evapotranspiration (crop growth based on EPIC model) and aquifer recharge (Neitsch et
159 al. 2002). The reference evapotranspiration method used in this study was the Penman-
160 Monteith method.
161 The nutrient component of the SWAT model includes inputs from agriculture, transport
162 with runoff and groundwater, consumption by plants and generation by mineralization in
163 the soil (Neitsch et al. 2002).
164 The SWAT model includes the main hydrological and nutrient processes occurring in a
165 watershed in order to describe the singularities of an extensive Mediterranean catchment
166 (flow temporality, crops, agricultural practices, etc.) and was implemented to quantify the
167 balance of the long-term dynamics and to estimate inflows to the Enxoé reservoir.
168

169 *2.3 Modeling approach*

170 As described above, the final objective in Enxoé is to link SWAT to a reservoir model to
171 describe the actual situation and produce scenarios that may be able to reduce the
172 reservoir trophic state. The work described here is for the watershed, where: i) the model
173 results are first validated against the data and ii) after model validation, the results are
174 extrapolated to the basin scale, presenting watershed dynamics and input loads to the
175 reservoir.
176 To implement and validate the model and produce useful information, field data need to
177 be integrated. The next chapters present the data used to implement and validate the
178 model and calibration procedure.
179

2.3.1 Data for model implementation

Table 1 shows the data used to implement the SWAT model to Enxoé (the digital terrain model, land use, soil texture, precipitation stations, climatic stations, etc.).

The land use map with SWAT classification is presented in Figure 2 and Table 2, where, as stated previously, olive trees (orchard), "montado" and annual crops each represent approximately 30% of the total area. The land use map was obtained from Corine 2000, and the aerial pictures and local observation show that the actual land use is still consistent with Corine map.

Information about annual crop agricultural practices (rotation and amount fertilized) was obtained from questionnaires given to farmers. The agricultural practices consist of rotation between wheat and oats in land use "annual crops rotation 2" in Figure 1 and rotation between sunflowers, wheat and oats in "annual crops rotation 1" (refer to Table 3 for the agricultural practice definitions for each crop). The annual input fertilization loads ranges were 40-90 $kgN.ha^{-1}.year^{-1}$ and approximately 20 $kgP.ha^{-1}.year^{-1}$.

The animal nutrient production was obtained from the 1999 national census data of the Statistical National Institute (INE) and is shown in Table 5. The annual animal loads were distributed homogeneously in oak and pasture sites (sheep and cattle) and in olive trees (sheep) because animal production is extensive in the watershed. The annual loads in animal production ranges were 6-30 $kgN.ha^{-1}.year^{-1}$ and 1-4 $kgP.ha^{-1}.year^{-1}$.

2.3.2 Data for model validation

Enxoé was an ungauged watershed in the river; thus, to define the state of the river and validate the model, data collection was performed during 2010-2011 in the two main

tributaries to the Enxoé reservoir (the Enxoé River and the river that passes through the only village, entering Enxoé before the beginning of the reservoir (Figure 1). The river data were collected on a weekly basis (with 3 samples collected each time) during the winter and the spring and when water existed during the summer (temporary river). The parameters evaluated in the laboratory were salinity, pH, nutrients, suspended solids, etc. In terms of flow validation, monthly data from Enxoé reservoir discharges and consumption, precipitation and evaporation were used to estimate the reservoir inflow (2006-2009).

Previous studies noted the importance of phosphorus in the reservoir and suggested studying its sources in more detail in the watershed. Furthermore, in the area (Alentejo), erosion is a major issue for agricultural activities (soil loss) because of the adverse effects on downstream water bodies. Therefore, erosion plots were installed for two of the main land uses (olive tree and "montado") to study erosion patterns and the data from these plots (areas around 60 to 900 m^2) are qualitatively compared with the SWAT results on erosion rates. The runoff volume and concentrations were sampled in the plots in weekly to monthly basis or after strong rain events.

Table 6 shows the data used for model validation (for flow and water quality).

2.3.3 Model evaluation

Both qualitative and quantitative measures were used to compare the observed data and the predicted values. Graphical analyses, such as time-series plots, were used to identify the general trends, potential sources of error, and differences between the measured and predicted values.

The SWAT model performance was evaluated using R^2 (the coefficient of determination that evaluates the correlation between two series), RMSE (the root mean squared error, which evaluates the deviation), and the Nash–Sutcliffe Efficiency (NSE) (the goodness-of-fit criterion for the predicated and observed values) (Nash and Sutcliffe, 1970). NSE values between 0.0 and 1.0 are generally viewed as acceptable levels of performance, whereas values <0.0 indicate that the mean observed value is a better predictor than the simulated value, which indicates unacceptable performance (Moriasi et al. 2007).

2.3.4 Model implementation and calibration procedure

For SWAT implementation, the data described above were introduced in the model interface AVSWAT for ArcView®, and the model was run using the SWAT 2005 executable version.

The SWAT model sensitivity analysis for discharge revealed that the most important parameters that impacted the results were CN2, Gwqmn, ESCO and SOL_AWC. However, the main difference between the hydrograph produced by the SWAT model with the default parameters and the real hydrographs measured in south Portugal in small-sized watersheds without known aquifer interactions, is that the SWAT model creates long baseflows that last for months after rain events and the peaks are usually lower in

SWAT. These results occur because the GW_DELAY and ALPHA_BF parameters, which control the travel timing of water between the soil and the aquifer and between the aquifer and the river, are unadjusted for small, temporary river watersheds in which travel times are small and hydrographs have a fast rise and fall correlated to rain events. The calibration procedure for hydrology consisted of changing the parameters GW_DELAY and ALPHA_BF as presented in Table 5. The values chosen were the same as those obtained via other SWAT projects in the same area (Alentejo) that compared the daily flow available (INAG, 2011 and other unpublished work) and were also of the same order as those used in works in temporary rivers in arid or semi-arid areas (e.g., the Meca River, Huelva, Spain, in Galvan et al. (2009) or the Gajwel watershed, India, in Perrin et al. (2012)).

In terms of the water quality, the river stream parameters were adjusted by trial and error to represent the behavior observed in the field data concentrations and loads. Although the initial total nitrogen and total phosphorus SWAT results were satisfactory when compared to these data, the first simulations exhibited excesses of organic nitrogen, ammonia and inorganic phosphorus and low nitrate concentrations, which drove the changes in the rates for mineralization between the organic and inorganic species described in Table 7. In addition, in the first simulations, nitrate and orthophosphate concentrations appeared to be associated only with rain events and their values were decreased to almost zero after an event, although field data concentrations remained higher throughout. The temporality and flushy flow regime shown in Figure 4 are consistent with observations and create long periods of low waters with increased retention times that have consequences for the river water quality and promote in-stream

processes, as observed in a similar-sized catchment in Alentejo in the work of Lillebø et al. (2007).

Enxoé is a small-sized, gently sloping (usually less than 5%) watershed with a 2% slope in the river. During low flow, the retention time increases drastically and pools tend to form, promoting deposition and making in-pool water quality processes relevant for estimating river concentrations (mineralization of deposited organic matter). The ammonia and dissolved phosphorus release from sediments used in the implementation and presented in Table 7 are important for estimating the dissolved phosphorus and nitrate concentrations in low-flow conditions, but these values do not have a significant impact on loads (10% increase in the total nitrogen and total phosphorus loads) because the majority of the loads are transported with rain events and high flow conditions.

SWAT uses a QUAL-2E formulation for the river quality, in which the phosphorus deposition is disconnected from the suspended sediment deposition, and the deposition and the release are not linked through a sediment state variable accounting for these fluxes. However, to maintain mass conservation, the results presented were verified so that the average annual deposition loads were higher than the release loads to assure consistency in the selected parameters.

3 Results and Discussion

3.1 SWAT model results: comparison with field data

The comparison between the SWAT model and the field data was made with respect to two different aspects: i) water inflow to the reservoir and ii) nutrient loads in the river.

293 The graphical comparisons are presented in the next sections and in Tables
294 Table 1, where it can be observed that in terms of the monthly flow or the monthly
295 nitrogen and phosphorus loads, the model adjustment to the data is satisfactory, with R^2
296 values higher than 0.60 (0.78 in flow) and Nash-Sutcliff efficiencies higher than 0.60
297 (0.77 in flow).
298

299 ### 3.1.1 Reservoir Inflow

300 The input flow to the reservoir has an important impact on the following: i) the reservoir
301 water volume and depth (the water quality in small depths tends to deteriorate because of
302 the availability of light at the bottom); ii) the retention time (increasing the retention time
303 increases the accumulation and time for algal assimilation of nutrients) and iii) the
304 horizontal and vertical mixing of water (intense mixing may deliver bottom nutrients to
305 the surface, where there is more light and a higher temperature). Therefore, describing the
306 input flow from the watershed is of major importance for driving reservoir dynamics.
307 The Enxoé watershed was an ungauged watershed; thus, to evaluate the SWAT results,
308 inflow to the reservoir was estimated tough a reservoir balance computation using
309 volume, discharge, precipitation and evaporation data for the period when all the
310 components were available (January 2006 to August 2009).
311 The comparison between the estimated inflow from the reservoir balance and the SWAT
312 model result is shown in Figure 3 and Tables
313 Table 1.
314 The time series comparison between monthly flows from the reservoir balance and the
315 SWAT model results (2006-2009) is presented at the top of Figure 3; the monthly

316 precipitation is presented on the reverse axis. The same values (from the data and the
317 model) are plotted on the x axis and the y axis at the bottom of Figure 3. Figure 3 shows
318 that both the model results and the estimates from the reservoir balance exhibit the same
319 trends (higher reservoir inflows in winter as a response to precipitation and a very low or
320 zero inflow in the summer in the absence of rain), as indicated by the R^2 value (0.78), and
321 are of the same order of magnitude, as indicated by the NS efficiency (0.77).
322 The results obtained for flow validation are comparable to those reported by Fohrer (2001)
323 in two watersheds in Hesse, Germany (R^2 of 0.71 and 0.92), Geza and McCray (2008) in
324 a 126 km^2 Turkey Creek watershed in Denver, USA (found an NSE of 0.61 and 0.70 and
325 R^2 of 0.62 and 0.74) and Green and van Griensven (2008) in small watersheds in Texas,
326 USA (obtained an NSE from 0.59 to 0.95 and R^2 from 0.60 to 0.96). In Mediterranean
327 countries, Dechmi et al. (2012) obtained high R^2 and NSE values of 0.90 in Del Reguero
328 River for a 20 km^2 watershed in northern Spain, while Panagopoulos et al. (2011) found
329 NSE values of 0.51 to 0.68 and an R^2 value of 0.86-092 in the Arachtos catchment (2000
330 km^2) in western Greece. In terms of the monthly flow, the present results fall in between
331 the results of other studies, showing that the SWAT model is able to represent the inflow
332 to the reservoir on a monthly scale.
333

334 ### 3.1.2 River sediment and nutrient loads

335 The last important aspects for accurately estimating affluences to the reservoir are the
336 input concentrations and loads.

Natural systems and organisms respond to the concentration (algae growth, etc.), but loads can give insights about the pressures that the reservoir is subjected to, which are especially important in cases of accumulation (e.g., suspended material and phosphorus). Nutrient concentrations (nitrate, ammonia, nitrite, organic nitrogen, total nitrogen, dissolved phosphorus, total phosphorus, etc.) were measured in Enxoé in 2010 and 2011 in two locations (see Figure 1), the Enxoé River and its main tributary, on a weekly basis; both stations were found to have similar concentrations, trends and values. There were no flow measurements in Enxoé, and flow estimation was only possible using a reservoir balance form 2006 to 2009, although the water quality data were collected in 2010 and 2011. Because the SWAT model produced satisfactory results in predicting the flow (2006-2009), loads from the measured data were computed using daily flow data from the SWAT model (2010-2011).

The Enxoé River represents approximately 75% of the total flow of the two tributaries. In Figure 4, the estimated flow during 2010-2011 is presented, and the precipitation is presented on the reverse axis. The river is dry or almost dry from June to October, and the first rain events (October and November) generate flow peaks that are quickly reduced (consistent with observations) because the soil is still not saturated and the groundwater flow is greatly reduced; from December/January to March, the response to the rain events still exists, but because the soil is saturated, baseflows are maintained longer but still tend to fall quickly, especially during months in which the total rain was less intense (e.g., January and February 2011).

A comparison between the total nitrogen monthly loads from the data and the SWAT model results (2009-2010) in the Enxoé River is presented at the top of Figure 5. The

same values (from the data and the model) are plotted on the x axis and the y axis with the x=y segment at the bottom of this figure. The same analysis is presented for total suspended sediments in Figure 6 and total phosphorus in Figure 7. Each sample from the river was collected in three different bottles and was independently analyzed in the laboratory to observe the natural variation and the sampling and laboratory variation. As so, the load based on the field data is graphed using dots to denote averages, and the maximum and minimum segment represents the maximum and minimum monthly load. As shown previously, the SWAT model gave satisfactory adjustments of the data in terms of the monthly flow, and similar behavior (with a lower fit) was observed with respect to the loads. Tables

Table 1 shows that the model estimate and loads based on the data are well correlated (R^2 of 0.69 for nitrogen and 0.63 for phosphorus) and have a similar order of magnitude (an NSE of 0.65 and 0.62 for nitrogen and phosphorus, respectively).

Sediment load

The model fit to the measured total suspended sediment loads has a lower rank than that for nitrogen and phosphorus because its R^2 is 0.42 and its NSE is 0.19. However, this result is highly dependent on the December 2010 value (approximately 8 tonSST/month in the model versus 1 tonSST/month from the data). Without this month the R^2 value would be 0.78 and the NSE would be 0.71, which is of the same order of magnitude as for the nitrogen and phosphorus loads. This difference may be attributable to underprediction of the field data or model overprediction. In fact, December 2010 was a month with several rain events, and a significant rain event occurred on 19/12/2010 that delivered 38 mm and generated the higher flow peak in Figure 4. In March 2011, heavy

rains and high flow peaks occurred, and the SWAT model was able to reproduce its high monthly load. Therefore, it was expected that December 2010 would produce a higher sediment load in the data, as SWAT estimated. The field data were collected three weeks before the event of 19/12/2010, and after the event, the next sample was taken in February. Therefore, the sampled total suspended solids concentrations in December 2010 may not be characteristic of the month, and some degree of underprediction linked to the data may be possible.

The December 2010 model overprediction may be attributable to overprediction on the same day (19/12/2010), when 7 tons of sediment was transported (of the total of 8 tons transported in this month). The high sediment load on this day resulted from the high peak runoff rates that the MUSLE equation generated. The SWAT model peak runoff rates are computed by a modified rational formula with the following form:

$$q_{peak} = \frac{\alpha_{tc} \cdot Q_{surf} \cdot Area}{3.6 \cdot t_c}$$

$$\alpha_{tc} = 1 - \exp\left[2 \cdot t_c \cdot Ln(1 - \alpha_{0.5})\right]$$

where:

q_{peak} is the MUSLE peak runoff rate ($m^3.s^{-1}$), α_{tc} is the fraction of the daily rainfall that occurred during the time of concentration (-), Q_{surf} is the surface runoff flow ($mm.h^{-1}$), Area is the HRU area (km^2), t_c is the concentration time (h) and $\alpha_{0,5}$ is the fraction of the daily rain at the highest half hour intensity (-).

For reduced values of the time of concentration (higher slopes in the watershed) and high values of the fraction of the daily rain at the highest half hour intensity, the peak runoff rate may be several times higher than the surface runoff, yielding artificial erosion rates.

405 Other authors have found a weaker fit to the data concerning sediment loads, such as
406 Dechmi et al. (2012) with respect to daily loads (an R^2 of 0.18); Panagopoulos (2011)
407 with respect to monthly loads, linking it to extrapolations in the field data (an NSE of
408 0.34 to 0.38); and Chu et al. (2004) in Warner Creek in Maryland, USA, with respect to
409 monthly loads (an R^2 of 0.19 and an NSE of 0.11), as a result of possible mispredictions
410 of the flow.
411 Aside from the overprediction in December 2010, as stated previously, the overall fit
412 when this month is removed is quite satisfactory, with an R^2 of 0.78 and an NSE 0.71;
413 these values are of the same order of magnitude as those of Dechmi et al. (2012) for
414 monthly loads (NSE of 0.52-0.72) and Gikas et al. (2005) in the Vistonis lagoon in
415 Greece (R^2 generally higher than 0.70 and up to 0.98 in 9 stations). The better fit is
416 consistent with the fact that the SWAT model predicted watershed average erosion rates
417 in 2010-2011 that were similar to the ones measured in the field erosion plots in that year.
418 As presented in Table 6, the experimental data and the model results are of the same
419 order of magnitude in erosion rates (0.1 to 0.4 $ton.ha^{-1}.year^{-1}$). The erosion plot results are
420 only used for indicative comparison because data only exist for one year.
421 The average annual erosion rate over all watershed and along the 30 year SWAT
422 simulation is 0.45 $ton.ha^{-1}.year^{-1}$, with some sub-basins producing values of up to 1 or 2
423 $ton.ha^{-1}.year^{-1}$. The work of Kosmas et al. (1997) investigated the land use effect on the
424 measured erosion rates in several Mediterranean watersheds and found erosion rates in
425 areas cultivated with wheat or olive groves (important land uses in Enxoé) of
426 approximately 0.01 to 0.2 $ton.ha^{-1}.year^{-1}$. In Roxo and Casimiro (1996), for Vale Formoso
427 erosion plots (Alentejo), values of approximately 2.5 $ton.ha^{-1}.year^{-1}$ were obtained, and in

Bakker et al. (2008), in which WaTEM/SEDEM was applied to Amendoeira (a watershed of the same size as Enxoé in Alentejo), values of 2 to 5 ton.ha^{-1}.year^{-1} were obtained; both of these studies reported values that were close to the maximum average values estimated by the SWAT model (the sub-basins with the higher slopes). These erosion rate values are low when compared to those of other studies concerning similar land uses with higher average slopes, such as in Vanwalleghem (2011), which reported an average slope of 25% in olive groves in 3 sites in Spain and erosion rates between 29 and 47 ton.ha^{-1}.year^{-1}. However, Enxoé has relatively gentle slopes (2% slope along the river and 5% average slope in SWAT sub-basins), and there are no significant differences between the headwaters and river valleys. The agriculture is extensive, and the simulated/measured erosion rates have similar values as those found in other studies for sites with similar land uses, slope and climate conditions.

Nutrient loads

Hydrology and suspended solids validation determine the main path of dissolved and particulate material, and hereafter the nutrients loads are evaluated against field data.

As stated above, the simulated nutrient loads show a good fit with the loads based on the measured concentrations during 2010-2011, with satisfactory correlation (an R^2 of 0.69 for nitrogen and 0.63 for phosphorus); furthermore, the simulated values are of the same order of magnitude as the measured data and yield satisfactory NSE values (0.65 and 062 for nitrogen and phosphorus, respectively).

The above results are in line with the results of other studies using the SWAT model. For example, for the total phosphorus monthly load, Dechmi et al. (2012) obtained an R^2 of 0.70-0.71 and an NSE of 0.63-0.66, whereas Green and van Griensven (2008) obtained

451 higher values for organic phosphorus and soluble phosphorus (R^2 of 0.72-0.78 and an
452 NSE of 0.5-0.78) and an R^2 of 0.7-0.8 and an NSE of 0.68 for nitrate and organic
453 nitrogen.
454 The analysis of the monthly total nitrogen and phosphorus loads presented in Figure 5
455 and Figure 7 showed, as expected, that the summer months have low or zero loads (July
456 to September 2010, when the flow is reduced or absent). In the beginning of winter or
457 spring, higher loads occur (rainy months), and the model is able to represent this trend as
458 seen in the above mentioned statistical parameters. However, the biggest difference
459 between the SWAT model loads and the loads based on field data occur in February and
460 March 2011, when the data present higher loads (differences of approximately 1
461 $tonN.month^{-1}$ and 0.05 $tonP.month^{-1}$) pointing to a underprediction of SWAT model load
462 in this two months. The concentrations in field data during these months are fairly stable,
463 and samples were not collected during flood events. Figure 4 shows that these months
464 have less precipitation events than October or December 2010 or March 2011 (namely,
465 the monthly precipitation in December is approximately 120 mm, that in January and
466 February is approximately 30 mm and that in March is approximately 60 mm) and
467 produce lower river flow peaks as a direct response; however, visible base flow is still
468 observable in these months because the soil was saturated in the previous months.
469 Because the surface water in February and March 2011 is reduced and base flow is
470 present, one could consider that in these months, the origin of the model underprediction
471 on load could be the lack of groundwater feeding and fertilization. However, this
472 underprediction would only affect the nitrate transport (phosphorus is retained in surface
473 and is hardly transported through soil or from groundwater to the river), but the

phosphorus load based on the data shows the same trend as the nitrogen load. Even tough, with SWAT model it was tested the amount of fertilization needed to achieve the order of magnitude of data nitrogen load in January and February 2011 and an unrealistic value of 500 kg mineralN.ha^{-1} was obtained because rain, infiltration, percolation and groundwater flow is not enhanced in this months since, as seen, rain is limited and also because vegetation is able to uptake the most part when amounts fertilized are not unrealistic.

With the groundwater feeding option discarded, one could then consider that the model underprediction could be explained by a lack on load being delivered by the surface water. There are two reasons why the load lacking was most likely not delivered by the surface water: i) the surface water is reduced in these months, as seen in Figure 4, by lower precipitation and lower flow peaks, and ii) the total suspended sediment load (transported by surface water) does not exhibit the same trend as the nitrogen and phosphorus loads and SWAT model is able to represent sediment load values. Even tough, fertilizations with mineral and organic forms were tested in SWAT model, and the effect was almost unobservable in January and February 2011 because of low surface water flows; however, the effect was quite visible in the following months and, thus, increased the estimated load and exceeded the field data.

If the model underprediction load in January and February 2011 did not originate from the surface or groundwater flow, then it must have originated from the river itself. As explained in the methodology section, the in-stream processes modeled by SWAT appear to be important for defining the order of magnitude of the sampled concentrations in low waters but cannot be used as an infinite source of nutrients; additionally, the source needed to obtain the field data load in these two months would generate abnormal loads

497 in the other months. Therefore, the process that generates an additional source of
498 nutrients may be mostly present in these months (January and February), and the
499 "culprits" in Enxoé could be the following: i) animal access to the river resulting in a
500 consequent direct nutrient source, and ii) the presence of a reed bed in the river bed. The
501 first source is unlikely to occur specifically in the referred months because animals are
502 present in the watershed throughout the year; moreover, these events are typically
503 followed by concentration peaks, specifically of ammonia, that are not verified in field
504 data (ammonia is low, and other nitrogen species are stable). As for the second source, in
505 Enxoé, the reed bed develops intensively (high density) inside the river sections upstream
506 and downstream of the sampling point where water is retained in pools or shallow
507 aquifers during the spring. These reed beds dry out during the summer and are dragged
508 downstream by high flows in the winter. The remaining roots inside the river bed may be
509 the organic matter source that promotes in-stream processes mainly after the first winter
510 months and enhances processes in months with lower flows, during which the residence
511 time increases (because of the occurrence of disconnected flow and pools), as may have
512 been the case in January and February 2011. As an auxiliary academic exercise, the reed
513 bed density needed to generate the field data loads in these two months was estimated by
514 assuming percentages of the root fraction from 10 to 50%, nitrogen percentages of 5 to
515 50% in these roots and phosphorus percentages of 1 to 10% in these roots (a wide range
516 of the SWAT model results for different crops). A density of 5 to 10 ton.ha^{-1} in the river
517 bed upstream of the sampling point was determined to be sufficient, which corresponds to
518 0.5 to 1 kg biomass per m^2. These amounts are quite reasonable (probably in Enxoé
519 higher) because in some areas it is not possible to see the river bed, while in other areas,

520 the occurrence is sparser. In the case of phosphorous, the nutrients needed to develop the
521 reed bed plants (i.e., the amount that may be mineralized in roots and generate the field
522 data loads) is less than the annual deposition load, whereas nitrogen could be available
523 from deposition and soil and groundwater nitrate pools. There is little information in the
524 literature about this subject (reed beds are used mostly in water treatment) and on the
525 modeling of such in-stream processes. The contributions of these processes do not
526 significantly impact the annual loads (they represent 10 to 20% of the annual load), but
527 because this is an open research subject, these in-stream processes should be studied in
528 more detail in the future in Enxoé using modeling tools with more advanced stream water
529 quality approaches.
530

531 **3.2. Enxoé watershed long-term budget**

532 After the comparison between the model simulation and the field data, the SWAT results
533 were used to extrapolate the watershed behavior to understand its dynamics in terms of
534 water and nutrient balance.
535 The water budget and the nitrogen annual average exports to the river are presented at the
536 top of Figure 8. Approximately 80-85% of precipitation (annual average in Enxoé is
537 approximately 500 mm) is evapotranspiration, and the remaining 15-20% is transported
538 to the river (10-15% by groundwater and lateral flow and 5% by runoff). Because of the
539 flush regime, runoff exports to the river carry 20 times more nitrogen (2.4-2.7 $kgN.ha^{-1}.year^{-1}$)
540 than groundwater (0.1 $kg.ha^{-1}.year^{-1}$).
541 A similar budget to that presented previously is also included at the bottom of Figure 8,
542 but in this budget, the annual averages of the suspended solids and phosphorus lost to the

543 river are shown. Phosphorus is mainly transported in runoff because inorganic forms of
544 phosphorus have the same charge as soil and are normally retained at the soil surface and
545 transported in runoff in dissolved, particulated or attached to fine soil particles (erosion).
546 The suspended solids export rate in Enxoé was estimated to be 0.45 ton.ha^{-1}.year^{-1},
547 whereas the phosphorus export rate was estimated to be 0.3 kg.ha^{-1}.year^{-1}.
548 The nutrient export values obtained in Enxoé are of the same order of magnitude as the
549 values obtained by Green and van Griensven (2008), who monitored small sub-basins
550 with mainly corn and wheat and less than 890 mm of annual precipitation in the USA and
551 found values of approximately 1 to 3 kgN.ha^{-1}.year^{-1} and 0.1 to 0.3 kgP.ha^{-1}.year^{-1}. The
552 nutrient export values obtained in Enxoé are also of the same order of magnitude as those
553 obtained by Alvarez-Cobelas et al. (2010), who used monitoring data from 3 semi-arid
554 sub-catchments in Spain with mainly vineyards and forest and annual precipitation of
555 approximately 400 mm and found values that ranged from 0.05 to 7 kgN.ha^{-1}.year^{-1} and
556 from 0.0004 to 1.6 kgP.ha^{-1}.year^{-1}. High nitrogen export tends to occur in areas where the
557 agriculture is more nutrient intensive and the annual precipitation is higher, promoting
558 nitrate leaching as, for example, in Central Europe (e.g., Salvia-Castellví et al. (2005)
559 studied field data in several Belgian watersheds and found nitrate exports of
560 approximately 27-33 kgN.ha^{-1}.year^{-1} in agricultural watersheds with annual precipitation
561 of approximately 700-1200 mm). On the other end, phosphorus exports tend to be higher
562 in areas with high erosion and can reach hundreds of kgP.ha^{-1} in a single event, as
563 described in Ramos and Mar -Casasnovas (2004) for a vineyard in northeast Spain.
564 The nutrient loads delivered to the Enxoé reservoir were estimated to be 18 tonN.year^{-1}
565 and 0.7 tonP.year^{-1} (30 year SWAT model simulation).

The Enxoé results concerning the exported nutrients to the reservoir are in the same range as other research results from extensive agricultural areas with gentle slopes (low erosion) and reduced human presence.

After the load is characterized in terms of the annual averages, the results can be shown also in terms of the temporal accumulation because high concentrations being transported in a short period of time is an important feature in temporary flushy regimes. In fact, the SWAT model results show that most of the annual nitrogen and phosphorus load (90% of the annual load) is delivered, on average, to the reservoir over approximately 15 days, while the sediment load is delivered over approximately 8 days (Table 8). These observations have already been described in the literature (e.g., González-Hidalgo et al. 2007), and the annual load "concentration" in a few events may have a significant impact on the reservoir.

Future work in Enxoé will involve the application of a reservoir model that will be fed by the loads estimated with this approach. Additionally, after the validation of the integrated watershed-reservoir approach with field data from the reservoir wall, management strategies will be tested to reduce the reservoir trophic state.

4 Conclusions

This work presented the first part of understanding the origin of the high eutrophic state of the Enxoé reservoir. The SWAT model was validated, and long-term inputs to the reservoir as well as sediment and nutrient exports were characterized.

The SWAT results were compared to the field data, and there was achieved satisfactory to good agreement with regard to the simulated flow and nutrient loads (monthly flow

589 with R^2 values and Nash-Sutcliffe efficiencies from 0.75 to 0.8 and nutrient loads from
590 0.62 to 0.70). The SWAT model application yielded similar fits to data as those reported
591 in other studies and was able to capture the main long-term trends and processes that
592 generate, transport and transform nutrients in the Enxoé watershed.
593 The results were extrapolated to the basin scale, and average annual values (30 year
594 simulation) revealed that approximately 80-85% of the annual precipitation
595 (approximately 500 mm) is evapotranspiration and that the remaining 15-20% is
596 delivered to the river. Moreover, nutrient exports to the river of nitrogen were on the
597 order of 2.5-2.8 $kg.ha^{-1}.year^{-1}$, suspended solids were 0.45 $ton.ha^{-1}.year^{-1}$ and phosphorus
598 was 0.3 $kg.ha^{-1}.year^{-1}$. The Enxoé results concerning exported nutrients to the reservoir
599 are in the same range as those of other studies of extensive agricultural areas with gentle
600 slopes (low erosion) and reduced human presence. The nutrient loads delivered to the
601 Enxoé reservoir were estimated to be 18 $tonN.year^{-1}$ and 0.7 $tonP.year^{-1}$ (30 year
602 simulation).
603 The average to low nutrient inputs from the watershed suggest that the high eutrophic
604 status in the reservoir may not be due only to input loads but also due to reservoir
605 geometry (average depth of 5 m), which results in high light availability at the bottom
606 where nutrient and organic matter accumulate (from watershed floods, deposition and
607 diagenesis), and the nutrient release to the water column may support the phytoplankton
608 communities. This hypothesis will be tested by integrating the SWAT model results into
609 a reservoir model to depict the origin of the Enxoé trophic status and test management
610 scenarios that may reduce it.

611 Because Enxoé is a small temporary watershed with a tendency toward a flushy regime
612 (almost 90% of the loads are transported over a period of 15 days annually) and in-stream
613 processes may have an important role on describing the nutrient concentrations in low
614 waters, two parallel research topics are suggested for future investigation: i) the role of
615 floods on watershed dynamics and weight on annual loads, and ii) detail the in-stream
616 and pool water quality processes occurring in low waters and discontinued flow.

Acknowledgments

The present work was supported within the framework of the EU Interreg SUDOE IVB program (SOE1/P2/F146 AguaFlash project), the Project Mirage (EU-FP7) and the Project EUTROPHOS (PTDC/AGR-AAM/098100/2008) of the Fundação para a Ciência e a Tecnologia (FCT).

References

Abbaspour, K.C.; Yang, J.; Maximov, I.; Siber, R.; Bogner, K.; Mieleitner, J.; Zobrist, J.; Srinivasan, R. (2007) - Modelling hydrology and water quality in the pre-alpine/alpine Thur watershed using SWAT, Journal of Hydrology, Volume 333, Issues 2–4, 15 February 2007, Pages 413-430, ISSN 0022-1694, 10.1016/j.jhydrol.2006.09.014.

Alvarez-Cobelas, M.; Sánchez-Andrés, R.; Sánchez-Carrillo, S.; Angeler, D.G. (2010) - Nutrient contents and export from streams in semiarid catchments of central Spain. Journal of Arid Environments, Volume 74, Issue 8, August 2010, Pages 933–945

Bakker, M. M.; Govers, G.; van Doorn, A.; Quetier, F.; Chouvardas, D.; Rounsevell, M. (2008) - The response of soil erosion and sediment export to land-use change in four areas of Europe: The importance of landscape pattern, Geomorphology, Volume 98, Issues 3–4, 15 June 2008, Pages 213-226, ISSN 0169-555X, 10.1016/j.geomorph.2006.12.027.

Carlson, R. E., (1977) - A trophic state index for lakes. Limnology and Oceanography, 22: 361-369.

640 Coelho, H.; Silva, A.; Chambel-Leitão, P.; Obermann, M. (2008) - On the origin of
641 cyanobacteria blooms in the Enxoé reservoir. Paper on 13th World Water Congress,
642 International Water Resources Association,. 1-4 September 2008 - Montpellier,
643 France.
644 Chu, T.W.; Shirmohammadi, A.; Montas, H.; Sadeghi, A.(2004) - Evaluation of the
645 SWAT model's and nutrient components in the piedmont physiographic region of
646 Maryland Trans. ASAE, 47 (5) (2004), pp. 1523–1538
647 Debele, B.; Srinivasan, R.; Parlange, J.-Y. (2005) - Coupling upland watershed and
648 downstream waterbody hydrodynamic and water quality models (SWAT and CE-
649 QUAL-W2) for better water resources management in complex river basins.
650 Springer Science + Business Media B.V. 2006.
651 Dechmi, F. Burguete, J. Skhiri, A. (2012) - SWAT application in intensive irrigation
652 systems: Model modification, calibration and validation, In Press - Journal of
653 Hydrology, Volumes 470–471, 12 November 2012, Pages 227-238, ISSN 0022-
654 1694, 10.1016/j.jhydrol.2012.08.055.
655 Fohrer, N; Eckhardt, K.; Haverkamp, S.; Frede, H.G. (2000). Applying the SWAT Model
656 as a Decision Support Tool for Land Use Concepts in Peripheral Regions in
657 Germany. Pages 994-999 Sustaining Global Farm. Papers from the 10th
658 International Soil Conservation Organisation Meeting.
659 Gallart, F.; Pérez-Gallego, N.; Latron, J.; Catari, G.; Martínez-Carreras, N.; Nord, G.
660 (2012) - Short- and long-term studies of sediment dynamics in a small humid
661 mountain Mediterranean basin with badlands, Geomorphology, Available online 9
662 June 2012, ISSN 0169-555X, 10.1016/j.geomorph.2012.05.028.

663 Galván, L.; Olías, M.; Fernandez de Villarán, R.; Domingo Santos, J.M; Nieto, J.M;
664 Sarmiento, A.M.; Cánovas, C.R. (2009) - Application of the SWAT model to an
665 AMD-affected river (Meca River, SW Spain). Estimation of transported pollutant
666 load, Journal of Hydrology, Volume 377, Issues 3–4, 30 October 2009, Pages 445-
667 454, ISSN 0022-1694, 10.1016/j.jhydrol.2009.09.002.
668 Geza, M.; McCray, J.E.(2008) - Effects of soil data resolution on SWAT model stream
669 flow and water quality predictions, Journal of Environmental Management, Volume
670 88, Issue 3, August 2008, Pages 393-406, ISSN 0301-4797,
671 10.1016/j.jenvman.2007.03.016.
672 Gikas, G.D.; Yiannakopoulou, T.; Tsihrintzis, V.A.(2005) - Modeling of nonpoint-source
673 pollution in a Mediterranean drainage basin. Environ. Model. Assess., 11 (3) (2005),
674 pp. 219–233.
675 Hidalgo, J. C. G.; Peña-Monné, J.L.; de Luis, M. (2007) - A review of daily soil erosion
676 in Western Mediterranean areas, CATENA, Volume 71, Issue 2, 15 October 2007,
677 Pages 193-199, ISSN 0341-8162, 10.1016/j.catena.2007.03.005.
678 Green, C.H.; van Griensven, A. (2008) - Autocalibration in hydrologic modeling: Using
679 SWAT2005 in small-scale watersheds. Environmental Modelling & Software 23
680 (2008) 422e434
681 Havens, K. E.; James, R. T.; East, T. L.; Smith, V. H. (2003) – N:P ratios, light limitation,
682 and cyanobacterial dominance in a subtropical lake impacted by non-point source
683 nutrient pollution. Environmental Pollution vol 122 pp 379-390.
684 INAG (2011) – Management of the trophic status in Portuguese reservoirs. Unpublished.

685 INAG (2004) – Plano de Ordenamento da Albufeira do Enxoé, estudos de caracterização
686 e pré-proposta de ordenamento. Management Plan for Enxoé Reservoir
687 (portuguese).
688 INE (2001) – Recenseamento Geral Agrícola 1999 RGA 1999. National Agricultural
689 Census 1999.
690 Kosmas, C.; Danalatos, N.; Cammeraat, L.H.; Chabart, M.; Diamantopoulos, J.; Farand,
691 R.; Gutierrez, L.; Jacob, A.; Marques, H.; Martinez-Fernandez, J.; Mizara, A.;
692 Moustakas, N.; Nicolau, J.M.; Oliveros, C.; Pinna, G.; Puddu, R.; Puigdefabregas,
693 J.; Roxo M.; Simao, A.; Stamou, G.; Tomasi, N.; Usai, D.; Vacca, A. (1997) - The
694 effect of land use on runoff and soil erosion rates under Mediterranean conditions,
695 CATENA, Volume 29, Issue 1, March 1997, Pages 45-59, ISSN 0341-8162,
696 10.1016/S0341-8162(96)00062-8.
697 Lam, Q.D.; Schmalz, B.; Fohrer, N. (2010) - Modelling point and diffuse source pollution
698 of nitrate in a rural lowland catchment using the SWAT model, Agricultural Water
699 Management, Volume 97, Issue 2, February 2010, Pages 317-325, ISSN 0378-3774,
700 10.1016/j.agwat.2009.10.004.
701 Lillebø, A.I.; Morais, M.; Guilherme, P.; Fonseca, R.; Serafim, A.; Neves, R. (2007) -
702 Nutrient dynamics in Mediterranean temporary streams: A case study in Pardiela
703 catchment (Degebe River, Portugal), Limnologica - Ecology and Management of
704 Inland Waters, Volume 37, Issue 4, 11 December 2007, Pages 337-348, ISSN 0075-
705 9511, 10.1016/j.limno.2007.05.002.
706 Mateus, V., Brito, D., Chambel-Leitão, P., Caetano, M. (2009) - Produção e utilização de
707 cartografia multi-escala derivada através dos sensores LISSIII, AWiFS e MERIS

708 para modelação da qualidade da água para a Bacia Hidrográfica do Rio Tejo.
709 Conferência Nacional de Cartografia e Geodesia, Caldas da Rainha, 7 e 8 de Maio
710 de 2009.
711 Ministry of Agriculture, (1997) – Código das Boas Práticas Agrícolas para a protecção da
712 água contra a poluição de nitratos de origem agrícola, GPP. Code on Best
713 Agriculture Practices, Ministry of Agriculture, 1997.
714 Moriasi, D.N.; Arnold, J.G.: Van Liew, M.W.; Bingner, R.L.; Harmel, R.D.; Veith, T.L.
715 (2007) - Model evaluation guidelines for systematic quantification of accuracy in
716 watershed simulations. Trans. ASABE 50 (3), 885–900.
717 Nasr, A.; Bruen, M.; Jordan, P.; Moles, P.; Kiely, G.; Byrne, P. (2007) - A comparison of
718 SWAT, HSPF and SHETRAN/GOPC for modelling phosphorus export from three
719 catchments in Ireland, Water Research, Volume 41, Issue 5, March 2007, Pages
720 1065-1073, ISSN 0043-1354, 10.1016/j.watres.2006.11.026.
721 Neitsch, S.L., Arnold, J.G., Kiniry, J.R., Srinivasan, R., Williams, J.R., (2002) - Soil and
722 Water Assessment Tool. User´s Manual. Version 2005. GSWRL Report 02-02,
723 BRC Report 2-06, Temple, Texas, USA.
724 OSPAR. (2001) - Draft Common Assessment Criteria and their Application within the
725 Comprehensive Procedure of the Common Procedure. Meeting of the
726 Eutrophication Task Group, London, 9 -11 October 2001, Annex5. Ospar
727 Convention for the Protection of the Marine Environment of the North-East Atlantic.
728 Paerl, H. W.; Fulton, R.S.; Moisander, P.H.; Dyble, J. (2001) – Harmful freshwater algal
729 blooms: with an emphasis on cyanobacteria. The Scientific World journal. Vol 1:
730 76-113.

731 Perrin, J.; Ferrant, S.; Massuel, S.; Dewandel, B.; Maréchal, J.C.; Aulong, S.; Ahmed, S.
732 (2012) - Assessing water availability in a semi-arid watershed of southern India
733 using a semi-distributed model, Journal of Hydrology, Volumes 460–461, 16
734 August 2012, Pages 143-155, ISSN 0022-1694, 10.1016/j.jhydrol.2012.07.002.
735 Panagopoulos, Y.; Makropoulos, C.; Mimikou, M. (2011) - Reducing surface water
736 pollution through the assessment of the cost-effectiveness of BMPs at different
737 spatial scales, Journal of Environmental Management Volume 92, Issue 10, October
738 2011, Pages 2823–2835
739 Rolff, C.; Almesjo, L.; Elmgren, R. (2007) - Nitrogen fixation and abundance of the
740 diazotrophic cyanobacterium Aphanizomenon sp. in the Baltic Proper. Marine
741 Ecology Progress Series vol. 332, pp 107-118.
742 -Casasnovas, J.A. (2004) - Nutrient losses from a vineyard soil in
743 Northeastern Spain caused by an extraordinary rainfall event. CATENA, Volume
744 55, Issue 1, 5 January 2004, Pages 79–90
745 Ramos, M.C.; Martínez-Casasnovas, J.A. (2006) - Nutrient losses by runoff in vineyards
746 of the Mediterranean Alt Penedès region (NE Spain). Agriculture, Ecosystems &
747 Environment, Volume 113, Issues 1–4, April 2006, Pages 356–363
748 Roxo, M.J.; Casimiro, P.C. (1997) - Long term monitoring of soil erosion by water Vale
749 Formoso Erosion Centre – Portugal; Soil Conservation and Protection for Europe
750 Project.http://eusoils.jrc.ec.europa.eu/projects/scape/uploads/97/Roxo_Casimiro.pdf
751 Salvia-Castellví, M.; Iffly, J.F.; Borght, P.V.; Hoffmann, L. (2005) - Dissolved and
752 particulate nutrient export from rural catchments: A case study from Luxembourg.

753 Science of The Total Environment, Volume 344, Issues 1–3, 15 May 2005, Pages
754 51–65
755 Saxton, K.E. et al. (1986) - Estimating generalized soil-water characteristics from texture.
756 Soil Sci. Soc. Amer. J. 50(4):1031-1036
757 UNL. (2003) - Estudo de Avaliação das Contribuições de Águas Residuais Urbanas nas
758 Albufeiras do Pocinho, Pracana, Maranhão e Vale do Gaio. Estudo Realizado no
759 Âmbito do Processo de Designação de Zonas Sensíveis em Águas Superficiais,
760 Directiva do Conselho 91/676/CEE, de 12 de Junho. Universidade Nova de Lisboa.
761 47 pp.
762 Valério, E.; Pereira, P.; Saker, M.L.; Franca, S.; Tenreiro, R. (2005) - Molecular
763 characterization of Cylindrospermopsis raciborskii strains isolated from Portuguese
764 freshwaters, Harmful Algae, Volume 4, Issue 6, November 2005, Pages 1044-1052,
765 ISSN 1568-9883, 10.1016/j.hal.2005.03.002.
766 Vanwalleghem, T.; Amate, J. I.; de Molina, M.G.; Fernández, D.S.; Gómez, J.A. (2011) -
767 Quantifying the effect of historical soil management on soil erosion rates in
768 Mediterranean olive orchards, Agriculture, Ecosystems & Environment,
769 Volume 142, Issues 3–4, August 2011, Pages 341-351, ISSN 0167-8809,
770 10.1016/j.agee.2011.06.003.
771 Vollenweider, R.A. (1976) - Advances in defining critical loading levels for phosphorus
772 in lake eutrophication. Memorie dell'Istituto Italiano di Idrobiologia, Vol 33: 53–83
773 Yevenes, M.A.; Mannaerts, C. M. (2011) - Seasonal and land use impacts on the nitrate
774 budget and export of a mesoscale catchment in Southern Portugal, Agricultural

775 Water Management, Volume 102, Issue 1, 15 December 2011, Pages 54-65, ISSN
776 0378-3774, 10.1016/j.agwat.2011.10.006.
777 Zhang, X., Srinivasan, R.; Van Liew., M. (2008) - Multi-Site Calibration of the SWAT
778 Model for Hydrologic Modeling, Transactions of the ASABE. 51(6): 2039-2049.

779 Tables

780 Table 1. Summary of the comparison of the SWAT model results to the collected data in

781 the Enxoé watershed.

Parameter	Period	Data average	Model Average	RMSE	R^2	Nash-Sutcliffe Efficiency
Flow						
Monthly Reservoir Inflow	1996-2009	0.24 $hm^3.month^{-1}$	0.24 $hm^3.month^{-1}$	0.21 $hm^3.month^{-1}$	0.78	0.77
Slope Erosion						
Annual erosion rates	2010-2011	0.1 - 0.2 $ton.ha^{-1}$	0.35 $ton.ha^{-1}$	-	-	-
River Water quality						
Monthly Total Nitrogen Load	2010-2011	0.62 $tonN.month^{-1}$	0.50 $tonN.month^{-1}$	0.46 $tonN.month^{-1}$	0.69	0.65
Monthly Total Suspended Solids Load	2010-2011	1.86 $tonTSS.month^{-1}$	1.80 $tonTSS.month^{-1}$	2.23 $tonTSS.month^{-1}$	0.42	0.19
Monthly Total Phosphorus Load	2010-2011	0.034 $tonP.month^{-1}$	0.030 $tonP.month^{-1}$	0.025 $tonP.month^{-1}$	0.63	0.62

782

783 Table 2. Description of the data for the SWAT model implementation in the Enxoé

784 watershed.

Data type	Description	Origin	Resolution	Period	Frequency
DTM	SRTM Digital Elevation	NASA	90 m	-	-
Land Use	Corine Land Cover 2000	EEA	1:100000	1999-2002	-
Soil Texture	European Soil database	JRC, EU	1:1000000	- 1996	-
Precipitation	Stations for daily input	SNIRH, National Water Institute (www.snirh.pt/)	-	1980-2011	Daily
Other Meteorology	Monthly averages for weather generator (1980-2000) and daily data (2000-2011)	National Meteorology Institute and SNIRH, National Water Institute (www.snirh.pt/)	-	Variant for monthly averages and 2000-2011 for daily data	Monthly averages and daily data after 2000

785

786

787

788

789

790 Table 3. Enxoé land use distribution areas (Source: Corine 2000).

Land Use	Area (km^2)	Percentage of total area
Olive trees	21	35%
Annual crops – Rotation 2	18	30%
Pasture/"Montado"	11	19%
Forest	7	11%
Annual crops – Rotation 1	2	3%
Water	1	2%
Urban area	<1	<1%
Total	61	100%

791

792 Table 4. Definitions of Enxoé agricultural practices (information collected from farmer

793 questionnaires).

Agricultural Practice	Crop Wheat and Barley	Oats	Sunflower	Olive Trees
Planting	November	October	April	-
Fertilization	November 20 kgN/ha November 18 kgP/ha January 50 kgN/ha February 20 kgN/ha	March 40-80 kgN/ha	April 22 kgP/ha	April to July (24-60 kgN/ha)
Harvest	June	June	September	-

794

795 Table 5. The number of animals in the Enxoé watershed (INE, 2001) and the annual

796 associated load (from per capita data from the Ministry of Agriculture, 1997).

Type	Number	Annual Load Nitrogen (tonN/year)	Phosphorus (tonP/year)
cattle	602	34	5
sheep	4365	78	13

797

798

799

800

801

802 Table 6. Description of the data for the SWAT model validation in the Enxoé watershed.

Data type	Station	Origin	Period	Frequency
Reservoir Inflow				
Reservoir Discharges	Enxoé Reservoir (26M/01A)	SNIRH, National Water Institute	2005-2009	Monthly
Precipitation	Herdade da Valada (26M/01C), Sobral Adiça (25N/01UG)	SNIRH, National Water Institute	1980-2011	Daily
Evaporation	Herdade da Valada (26M/01C), Monte da Torre	SNIRH, National Water Institute	2001-2011	Daily
Erosion				
Erosion rates	Two plots in two main land uses. Volume and solids concentrations collected	Project	2010-2011	Weekly to monthly
Water quality in river				
Nutrient	Two stations in the two main tributaries	Project	2010-2011	Weekly to monthly

803

804 Table 7. SWAT model parameter calibration in the Enxoé watershed.

Parameter Description	SWAT name	SWAT file	Default Value	Calibrated Value
Hydrodynamic				
Groundwater delay (days)	GW_DELAY	.gw	31	3
Base flow recession alpha factor (days)	ALPHA_BF	.gw	0.048	1
Water Quality				
Linear parameter for calculating the maximum amount of sediment that can be reentrained during channel sediment routing	SPCON	.bsn	0.0001	0.00005
Organic phosphorus settling rate in the reach at 20ºC [day-1]	RS5	.swq	0.05	0.35
Benthic (sediment) source rate for dissolved phosphorus in the reach at 20ºC (mg dissolved P/(m^2·day))	RS2	.swq	0.05	0.5
Benthic source rate for NH_4-N in the reach at 20ºC (mg NH_4-N/(m2·day))	RS3	.swq	0.5	10
Rate constant for hydrolysis of organic N to NH4 in the reach at 20º C (day-1)	BC3	.swq	0.21	0.25
Rate constant for biological oxidation of NH_4 to NO_2 in the reach at 20º C (day-1)	BC1	.swq	0.55	2.0
Rate constant for biological oxidation of NO_2 to NO_3 in the reach at 20º C (day-1]	BC2	.swq	1.1	3.0
Rate constant for mineralization of organic P to dissolved P in the reach at 20º C (day-1)	BC4	.swq	0.35	0.01

805

806 Table 8. SWAT model result of the number of days to achieve 90% of the annual load

807 transported on the Enxoé river to the reservoir (1980-2010 results).

	Nº of days to transport 90% of annual load		
	Total Nitrogen	Total Phosphorus	Suspended Sediment
Average	12	14	8
Maximum	28	27	23
Minimum	1	1	1

808

809

Figure Captions

Figure 1. Location of the Enxoé study area and monitoring stations. The Digital Elevation Model (Source: NASA) and the drainage network are also presented.

Figure 2. The Enxoé land use distribution map (Source: Corine 2000). The Enxoé Reservoir and drainage network are also presented.

Figure 3. The monthly inflow to the Enxoé reservoir: a comparison between the estimate from the reservoir balance and the simulation from the SWAT model. Top –a flow comparison per month; the monthly precipitation is also presented on the inverted secondary axis. Bottom – a flow comparison on both the axis and the segment y = x (perfect fit) is presented.

Figure 4. The Enxoé river estimated SWAT flow during 2010-2011, when the water quality data were collected. The daily precipitation is also presented on the inverted secondary axis.

Figure 5. The Enxoé river total nitrogen load: a comparison between estimates from the field data and the SWAT model results. Top – a load comparison per month; Bottom – a load comparison on both the axis and the segment y = x (perfect fit).

Figure 6. The Enxoé river total suspended solids concentrations: a comparison between the field data and the SWAT model results. Top – a load comparison per month; Bottom – a load comparison on both the axis and the segment y = x (perfect fit) is presented.

Figure 7. The Enxoé river total phosphorus load: a comparison between estimates from the field data and the SWAT model results. Top – a load comparison per month; Bottom – a load comparison on both the axis and the segment y = x (perfect fit) is presented.

832 Figure 8. The Enxoé watershed annual average water and nutrient balance and export to
833 the river. Top – the water and nitrogen annual averages; Bottom – the water and
834 phosphorus annual averages.

835 Figure 1

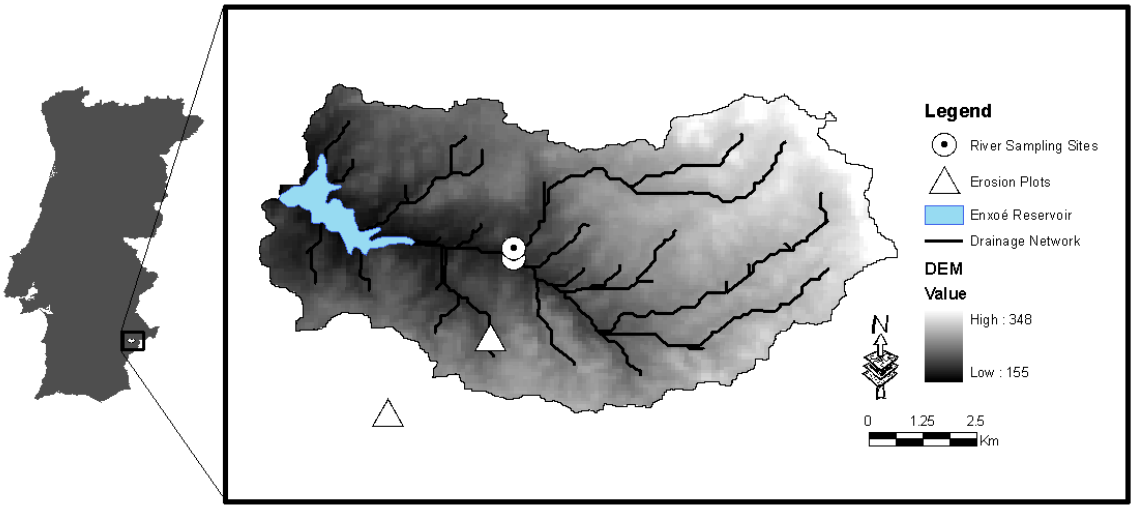

836

837

838 Figure 2

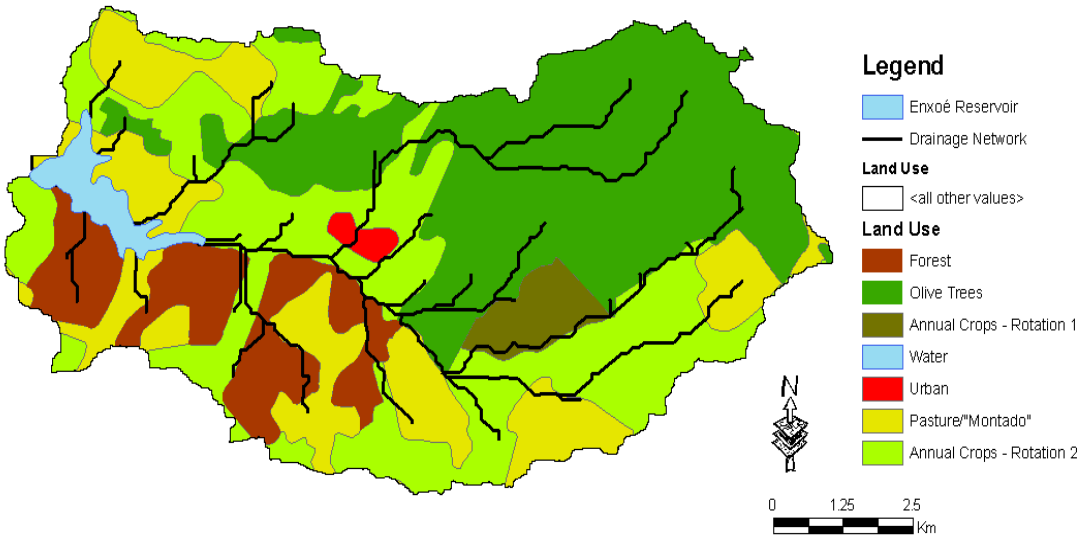

839

840

841 Figure 3

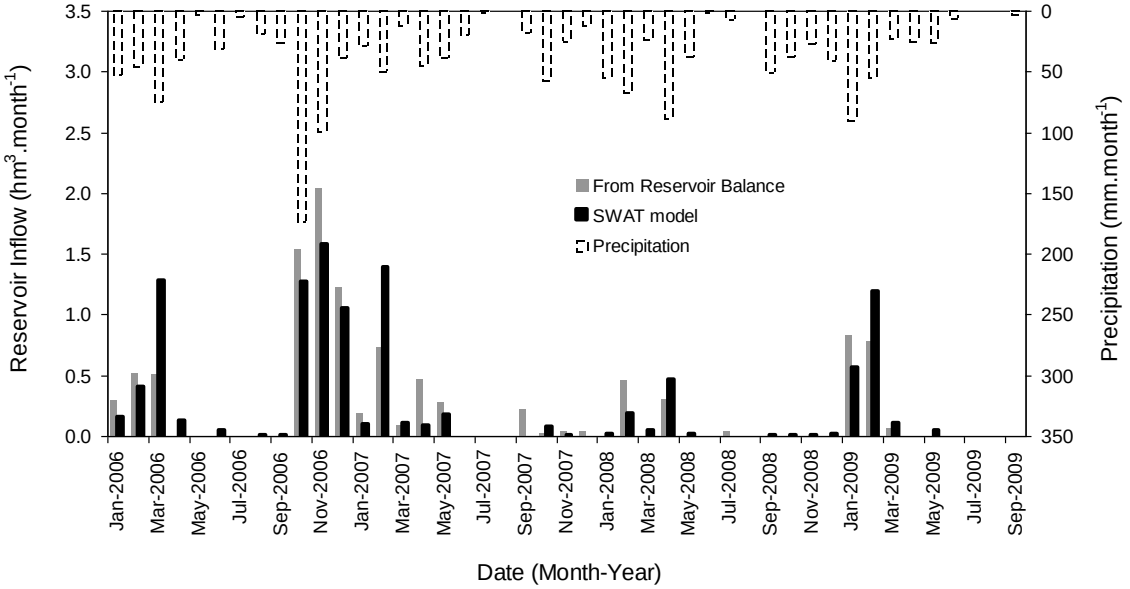

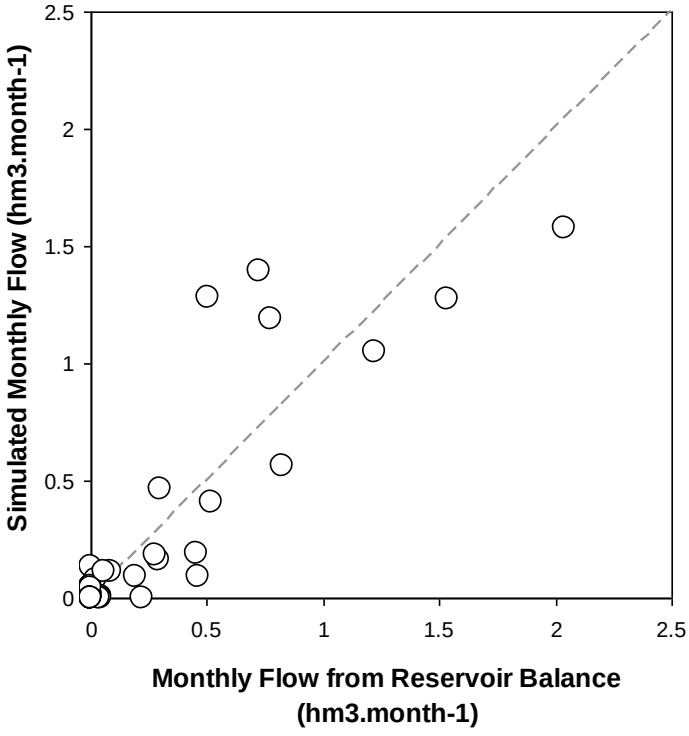

842

843

844

845 Figure 4

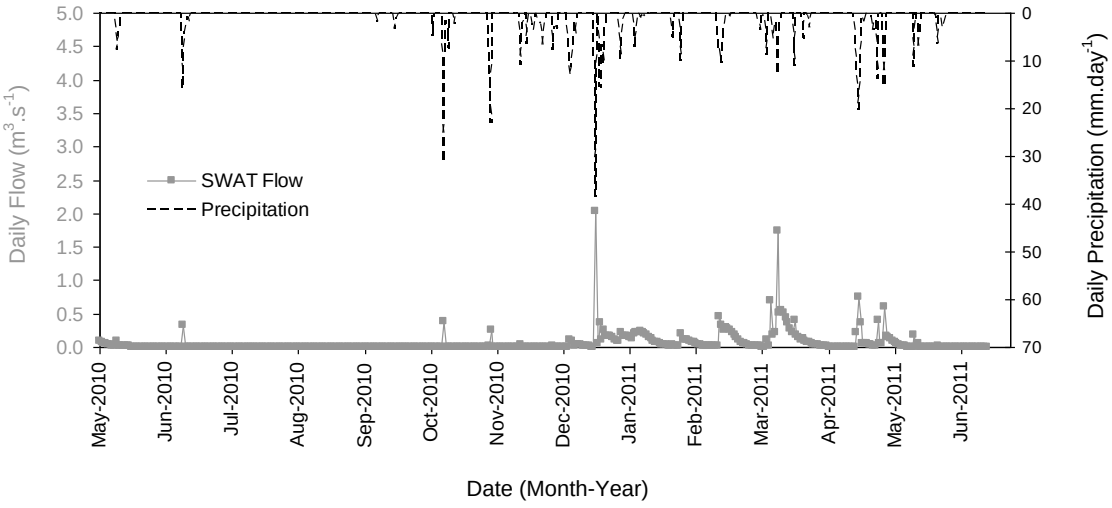

846

847

848

849

850

851

852

853

854

855

856

857

858

859

860 Figure 5

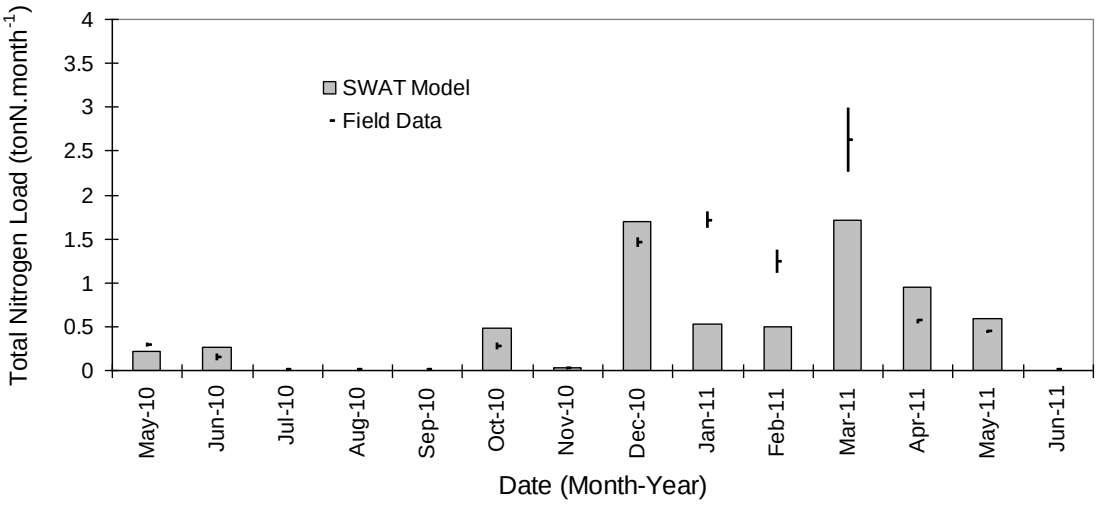

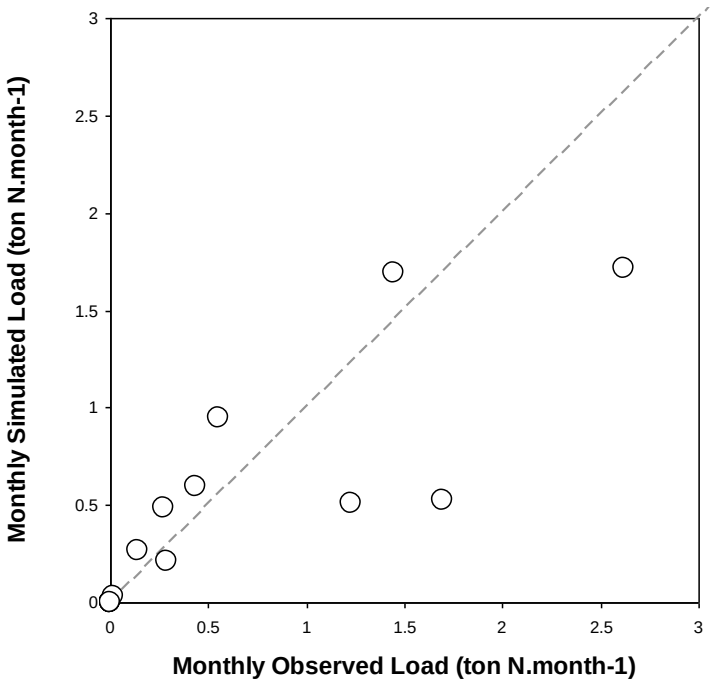

861

862

863

864

865 Figure 6

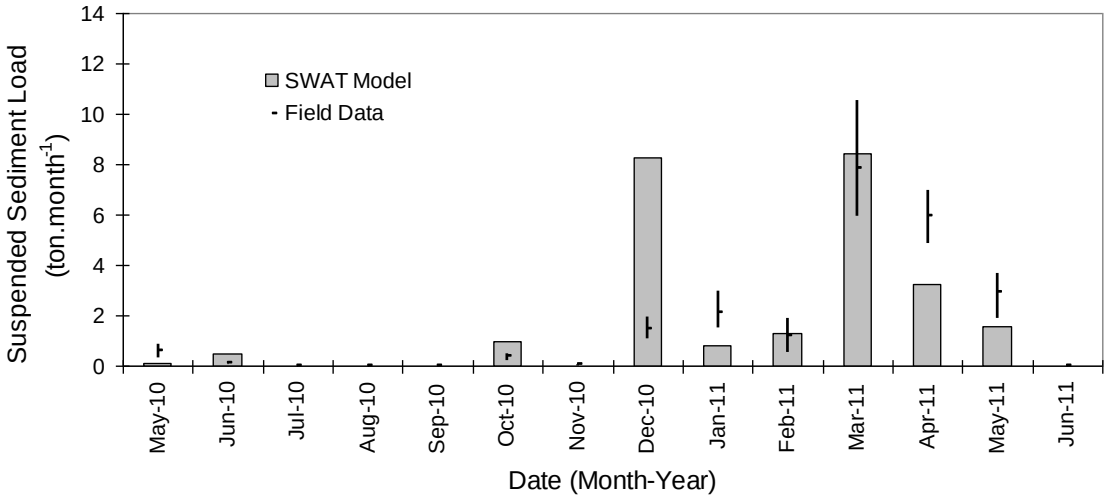

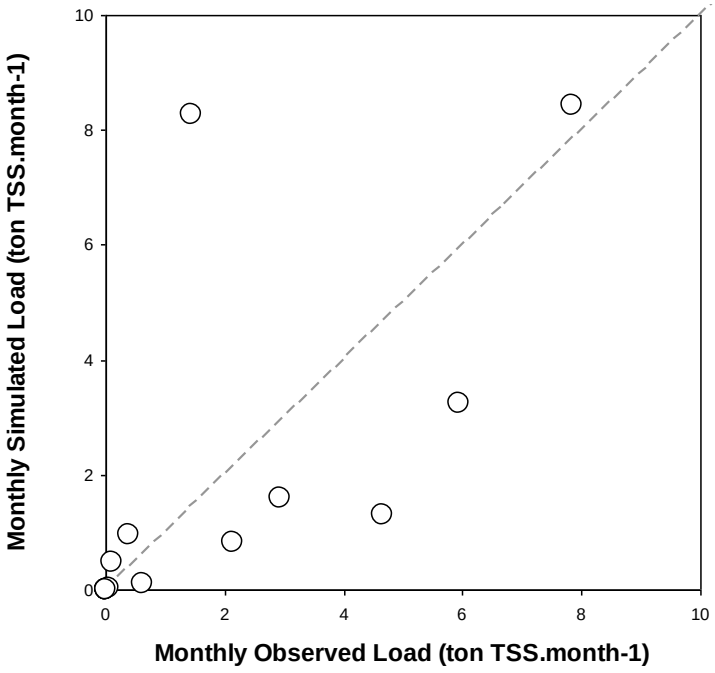

866

867

868

869

870 Figure 7

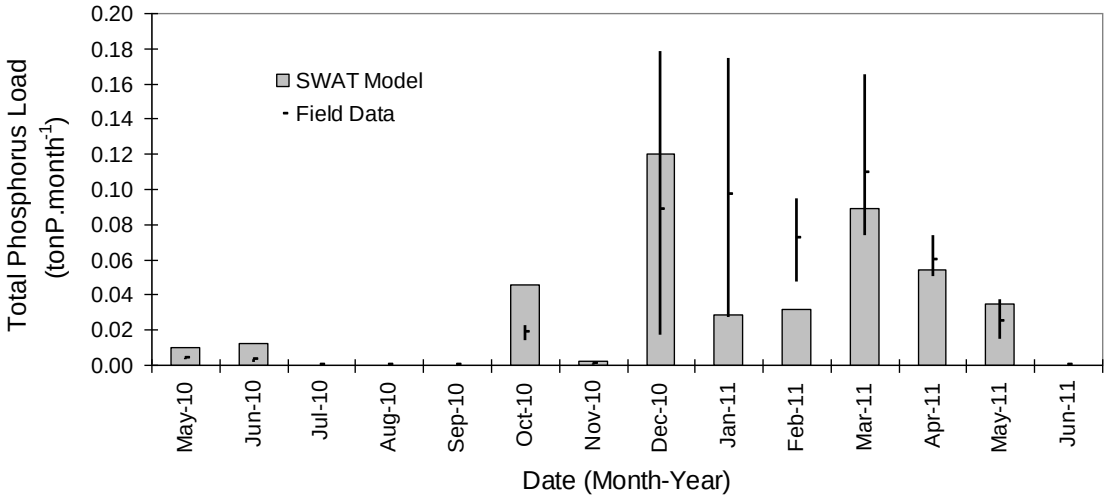

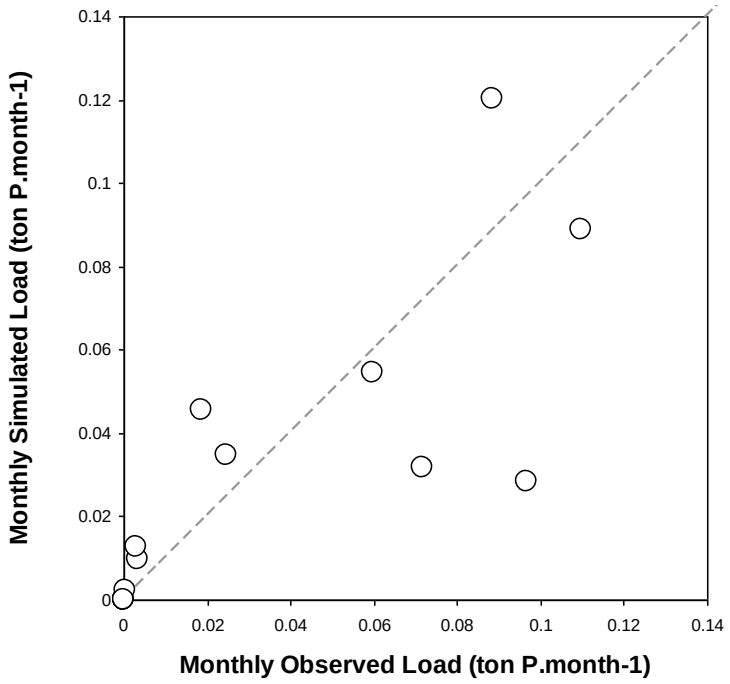

871

872

873

874

875 Figure 8

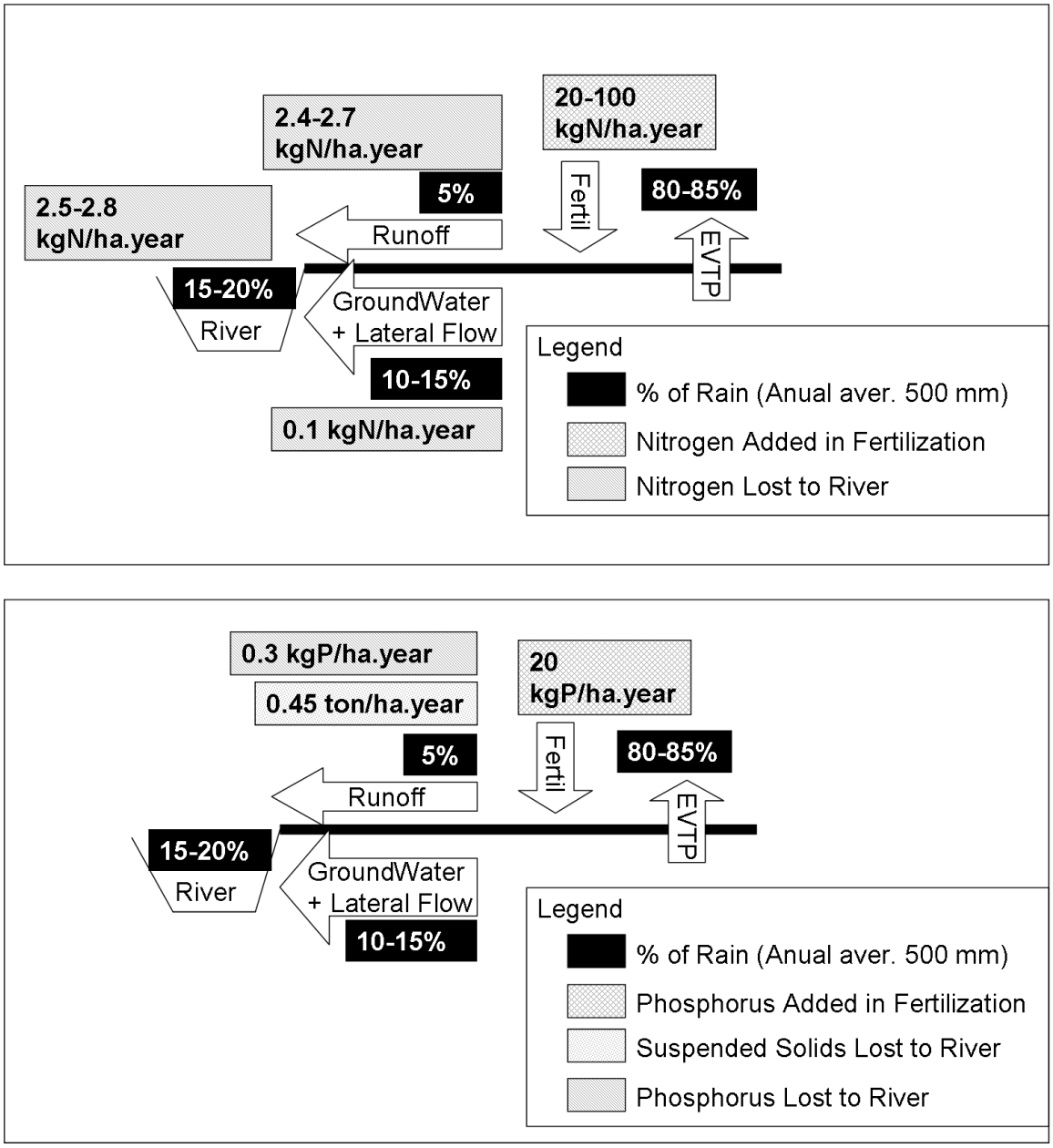

876

Highlights:

- Applied SWAT model to quantify long-term nutrient loads to a eutrophic reservoir.
- SWAT adjusted well to measured monthly reservoir input flow and nutrient loads.
- Long-term watershed nutrient loads are low and consistent with field data.
- Eutrophication may link to reservoir geometry and modeling framework is suggested.

Figure Captions

Figure 1. Location of the Enxoé study area and monitoring stations. The Digital Elevation Model (Source: NASA) and the drainage network are also presented.

Figure 2. The Enxoé land use distribution map (Source: Corine 2000). The Enxoé Reservoir and drainage network are also presented.

Figure 3. The monthly inflow to the Enxoé reservoir: a comparison between the estimate from the reservoir balance and the simulation from the SWAT model. Top –a flow comparison per month; the monthly precipitation is also presented on the inverted secondary axis. Bottom – a flow comparison on both the axis and the segment y = x (perfect fit) is presented.

Figure 4. The Enxoé river estimated SWAT flow during 2010-2011, when the water quality data were collected. The daily precipitation is also presented on the inverted secondary axis.

Figure 5. The Enxoé river total nitrogen load: a comparison between estimates from the field data and the SWAT model results. Top – a load comparison per month; Bottom – a load comparison on both the axis and the segment y = x (perfect fit).

Figure 6. The Enxoé river total suspended solids concentrations: a comparison between the field data and the SWAT model results. Top – a load comparison per month; Bottom – a load comparison on both the axis and the segment y = x (perfect fit) is presented.

Figure 7. The Enxoé river total phosphorus load: a comparison between estimates from the field data and the SWAT model results. Top – a load comparison per month; Bottom – a load comparison on both the axis and the segment y = x (perfect fit) is presented.

Figure 8. The Enxoé watershed annual average water and nutrient balance and export to the river. Top – the water and nitrogen annual averages; Bottom – the water and phosphorus annual averages.

Figure1.tif
Click here to download high resolution image

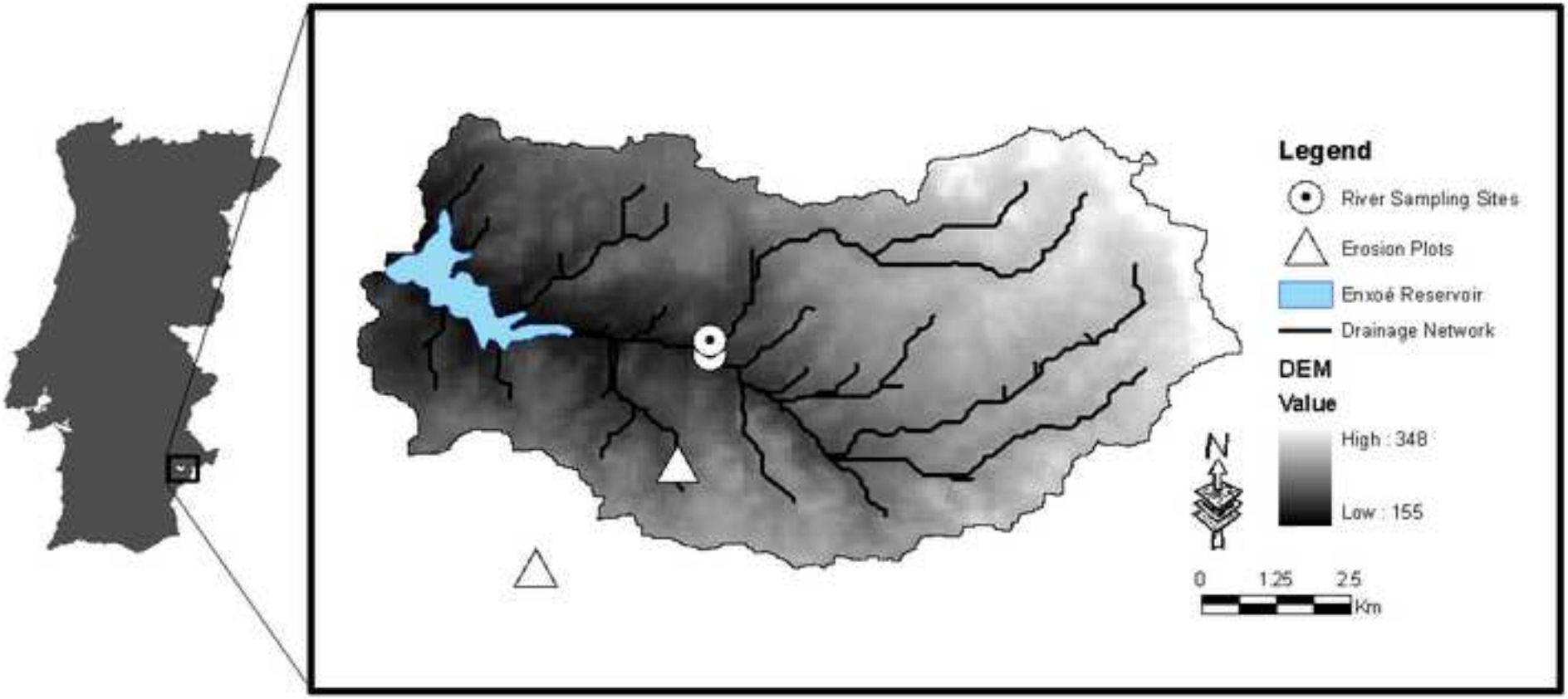

Figure2.tif
Click here to download high resolution image

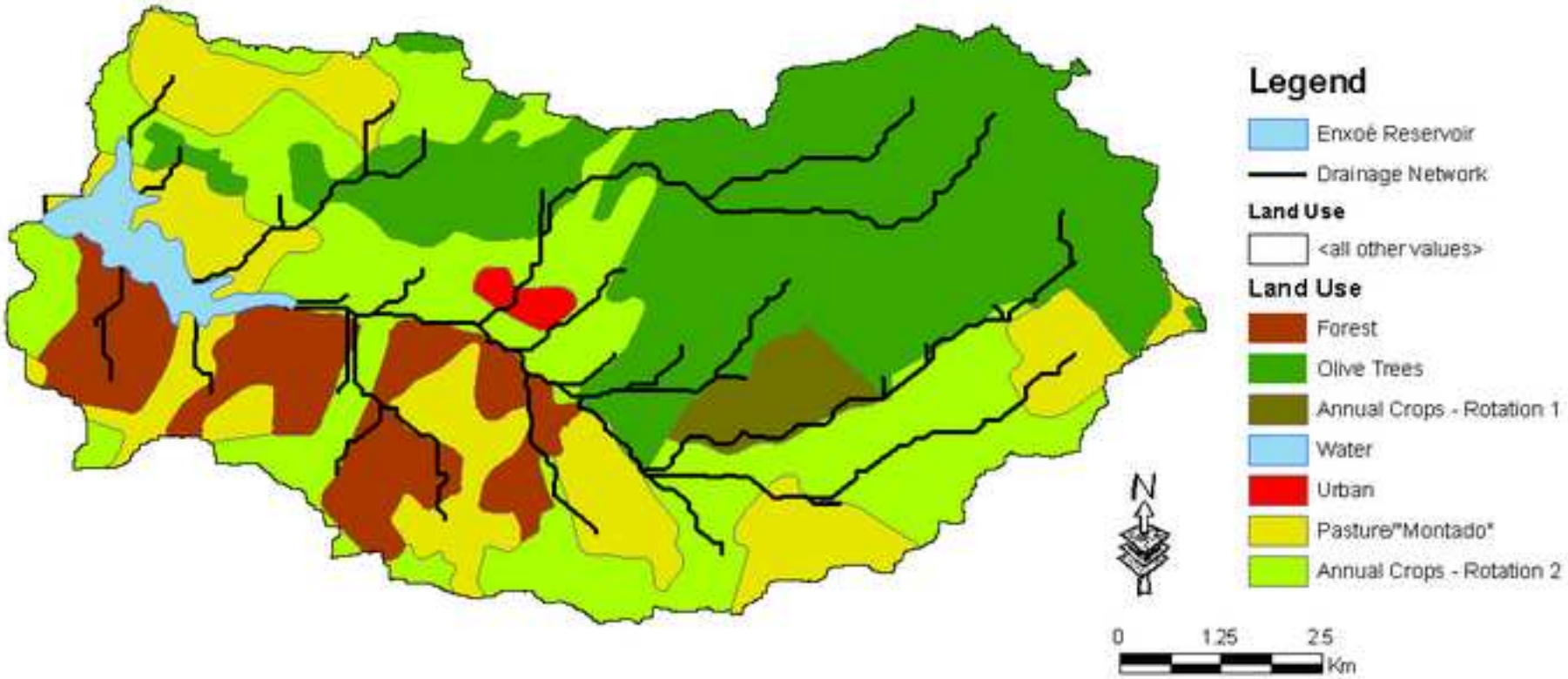

Figure2_B&W.tif
Click here to download high resolution image

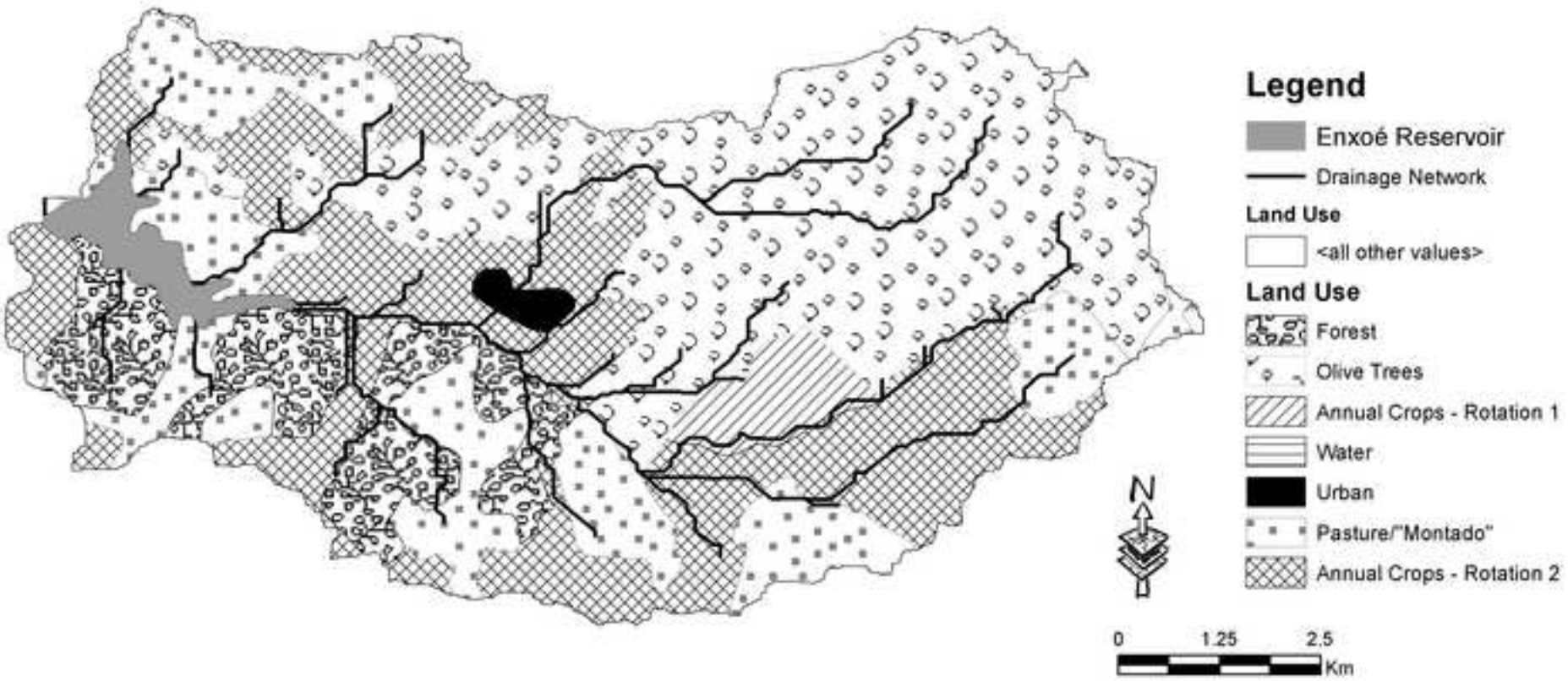

Figure3a.TIF
Click here to download high resolution image

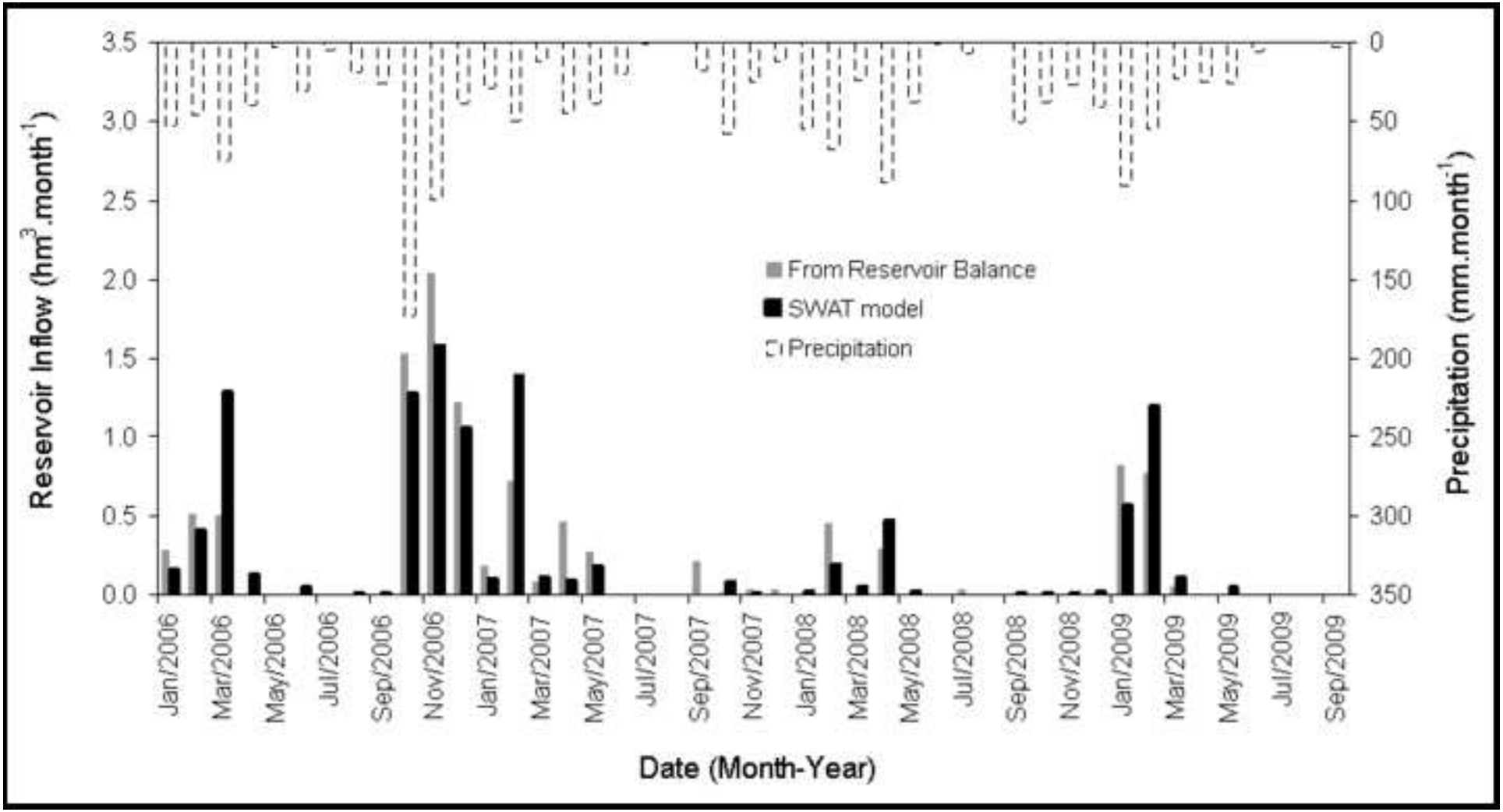

Figure3b.TIF
Click here to download high resolution image

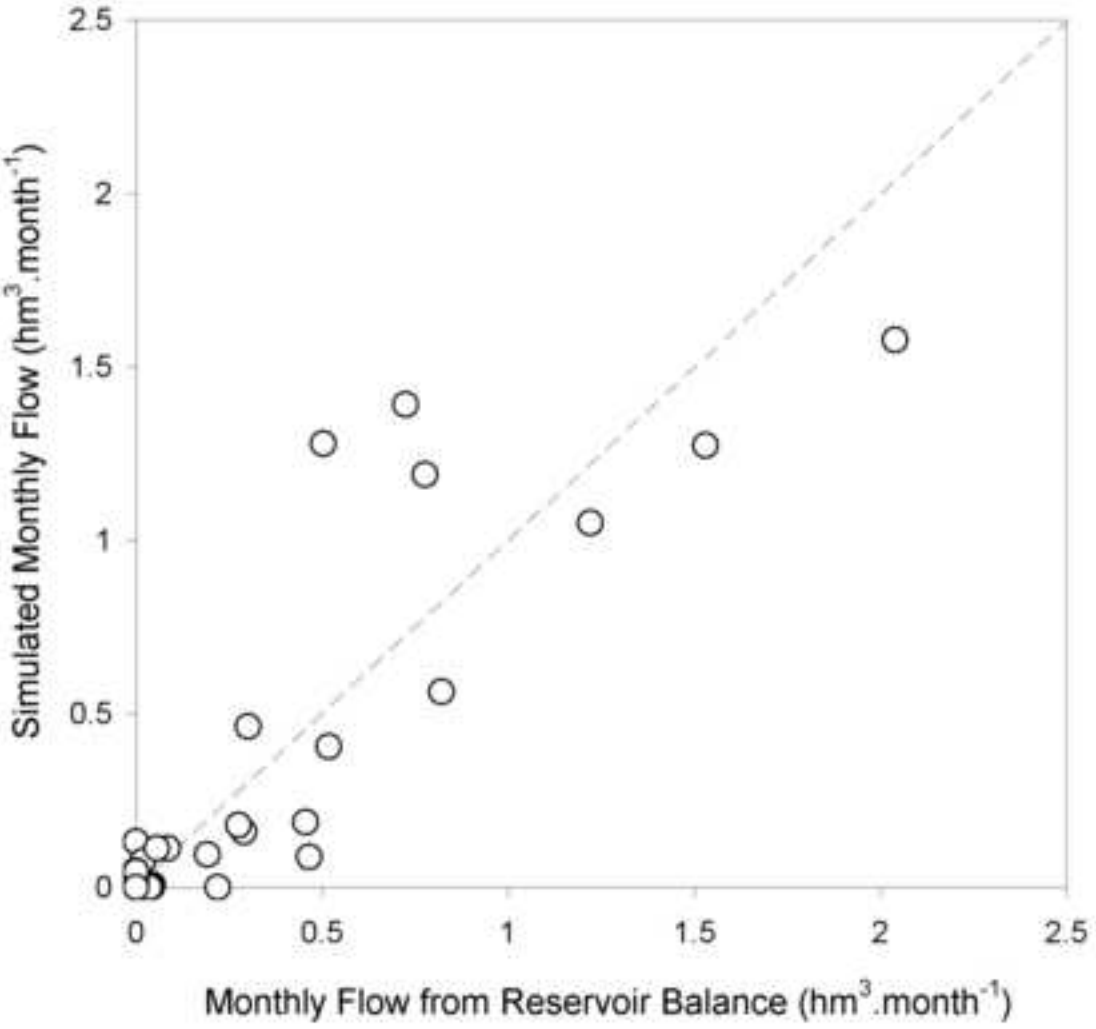

Figure4.TIF
Click here to download high resolution image

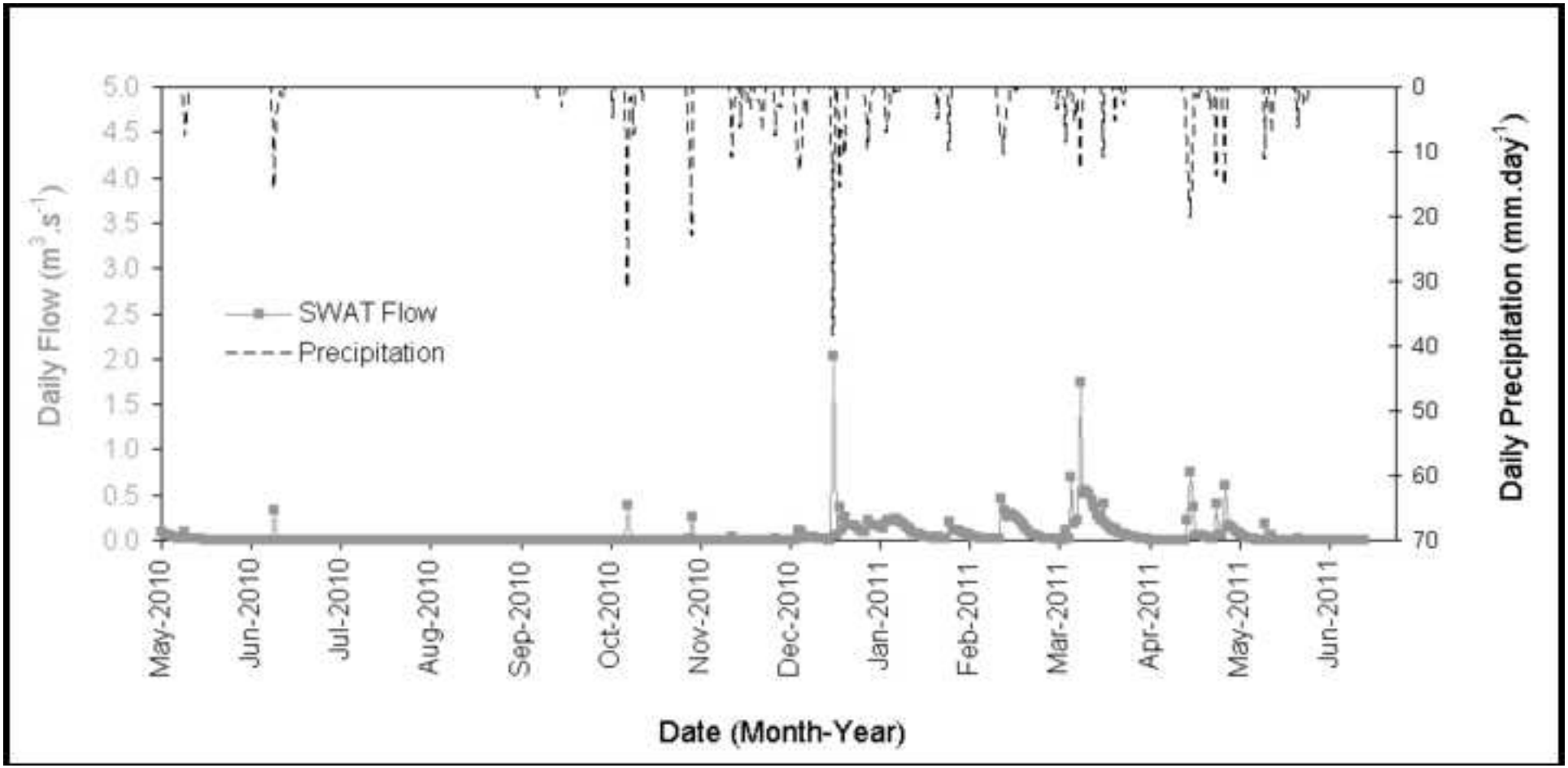

Figure5a.TIF
Click here to download high resolution image

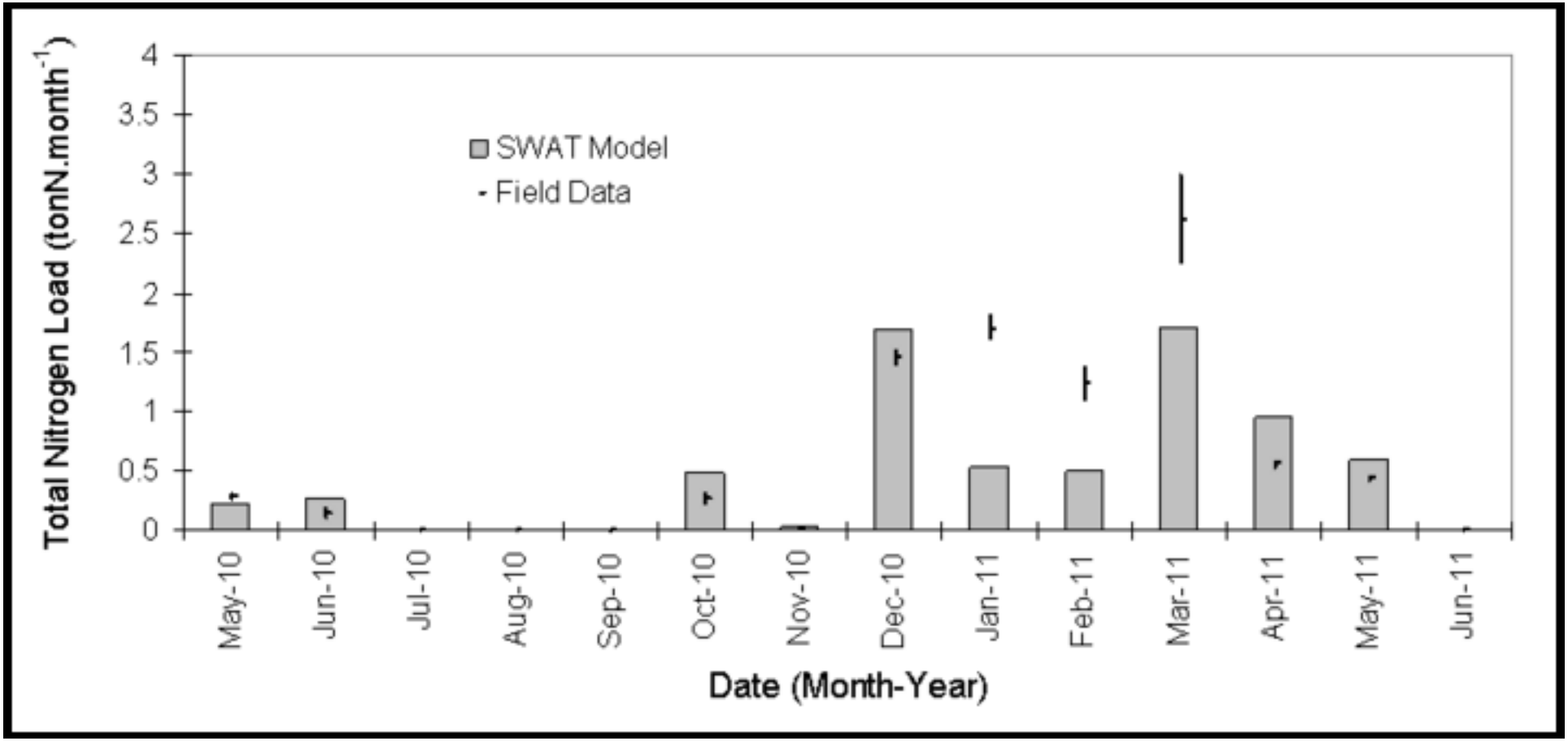

Figure5b.TIF
Click here to download high resolution image

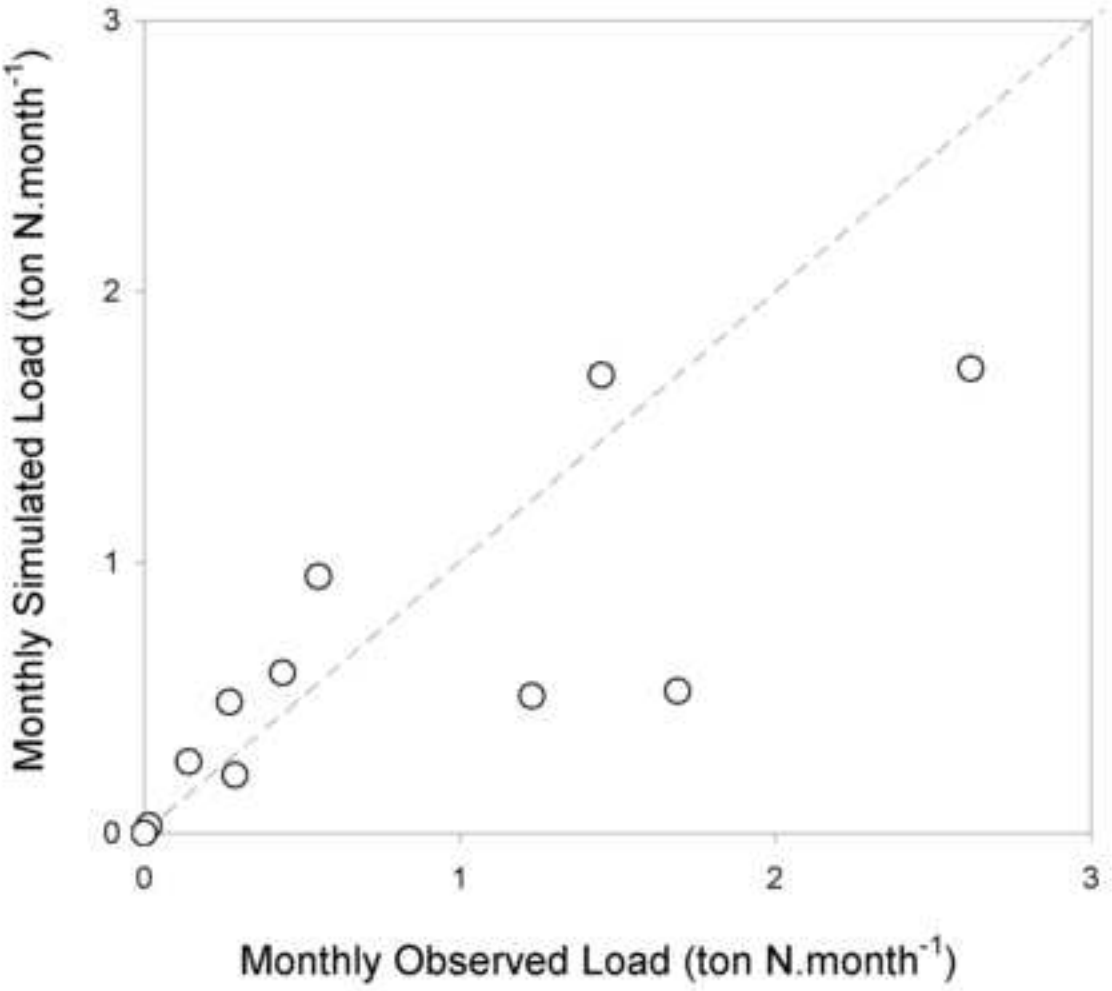

Figure6a.TIF
Click here to download high resolution image

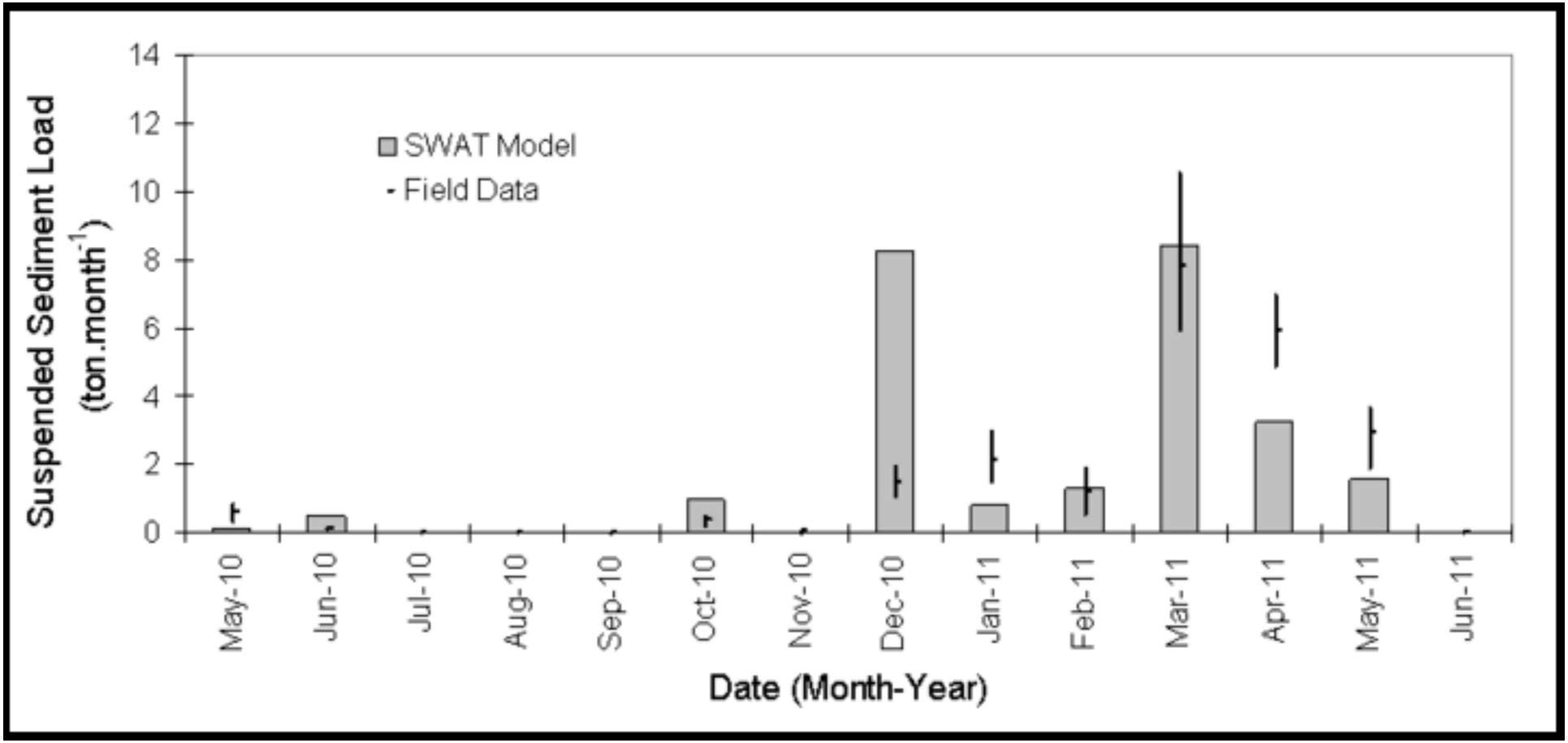

Figure6b.TIF
Click here to download high resolution image

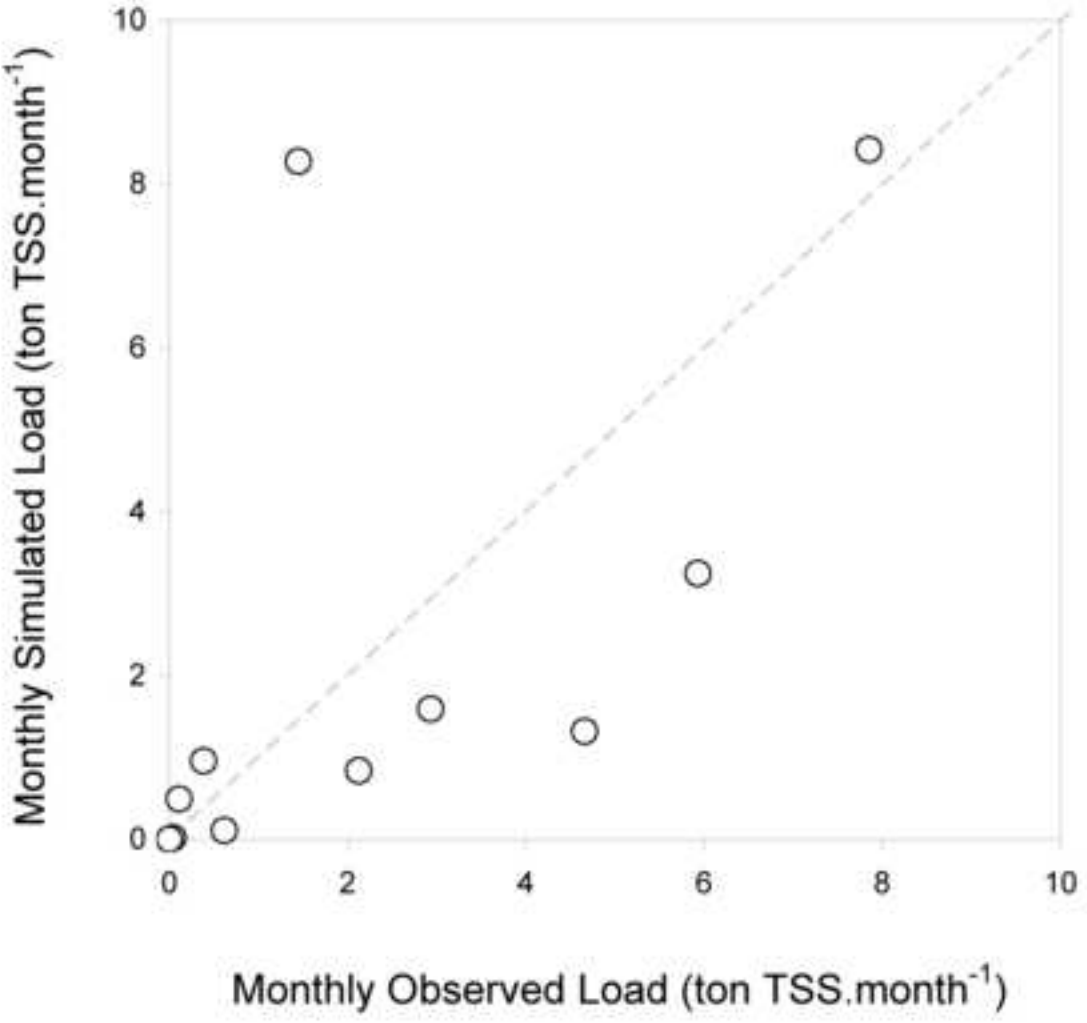

Figure7a.TIF
Click here to download high resolution image

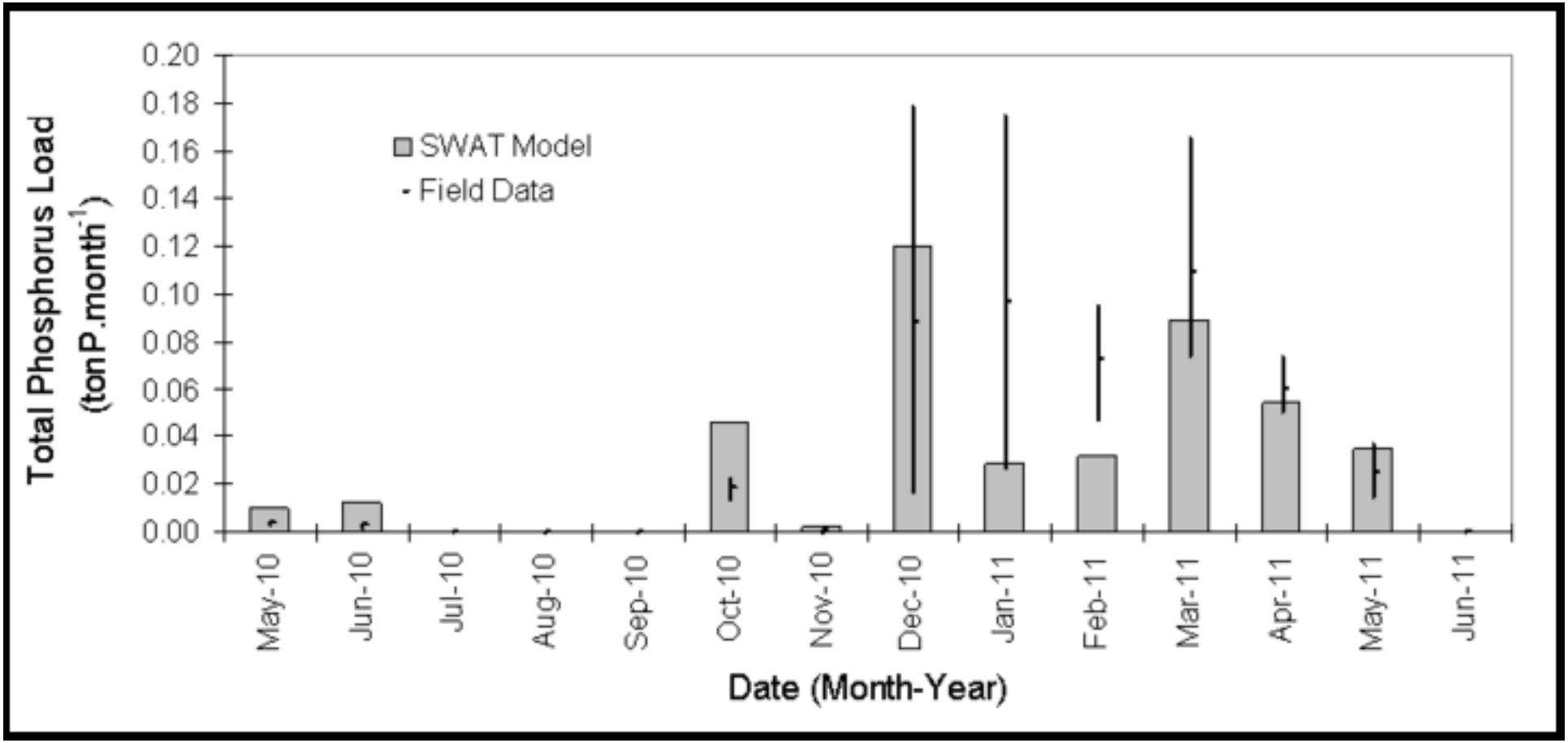

Figure7b.TIF
Click here to download high resolution image

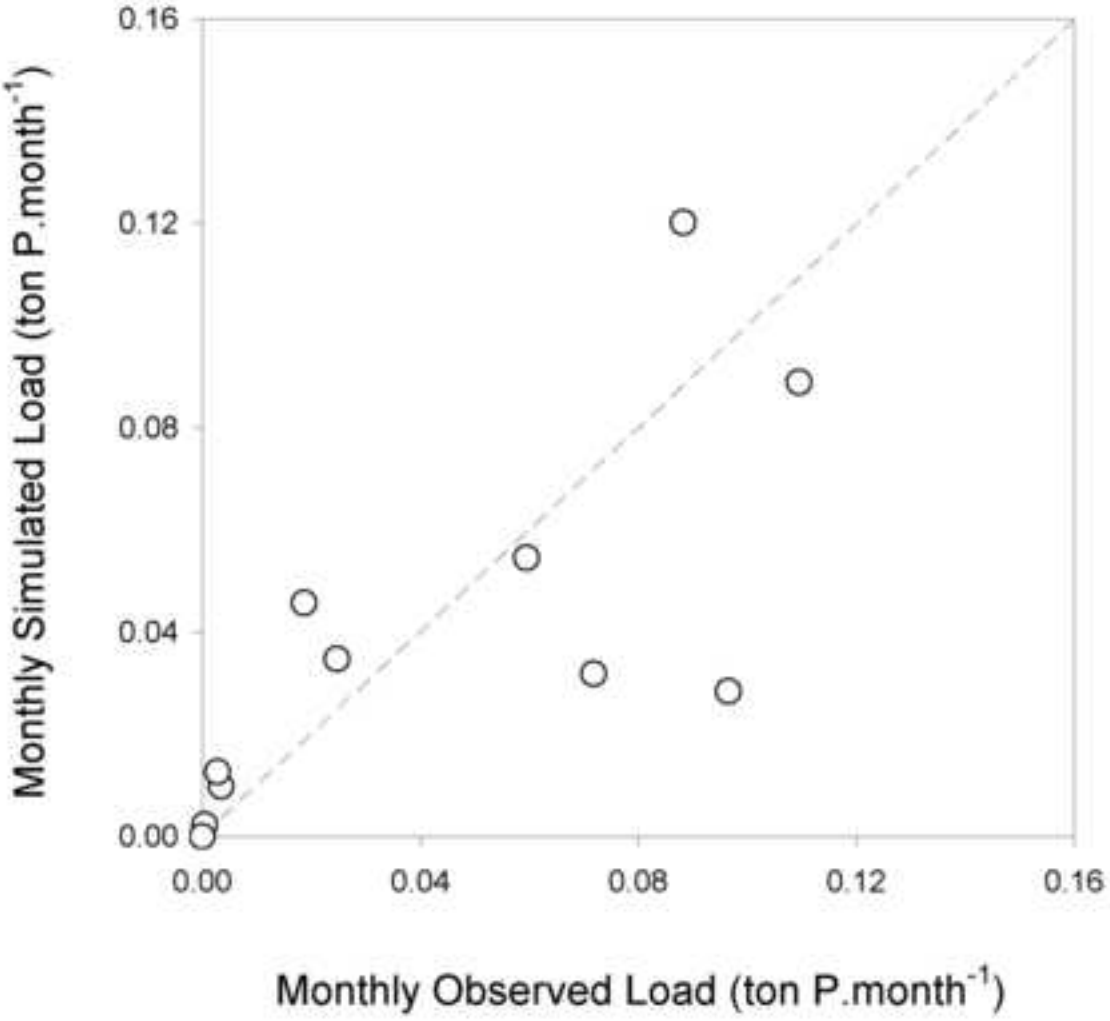

Figure8a.tif
Click here to download high resolution image

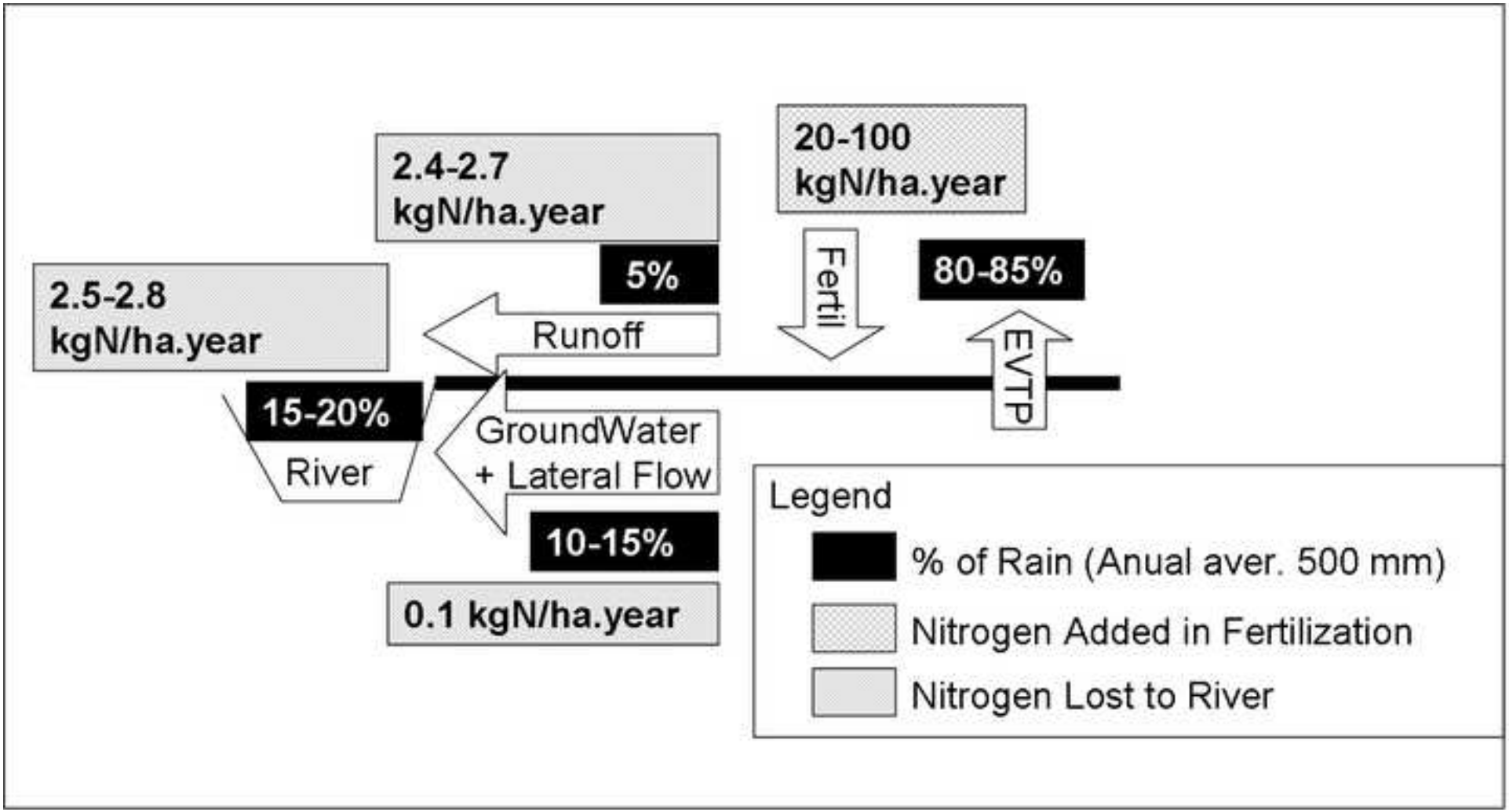

Figure8b.tif
Click here to download high resolution image